LOCKHEED MARTIN ENERGY RESEARCH LIBRARIES
3 4456 0513079 2

CENTRAL RESEARCH LIBRARY
DOCUMENT COLLECTION
1

OAK RIDGE NATIONAL LABORATORY
operated by
UNION CARBIDE CORPORATION
NUCLEAR DIVISION
for the
U.S. ATOMIC ENERGY COMMISSION

ORNL-TM-2263

PHYSICAL AND MECHANICAL PROPERTIES OF TYPE 406 STAINLESS STEEL

H. E. McCoy, Jr.

OAK RIDGE NATIONAL LABORATORY
CENTRAL RESEARCH LIBRARY
DOCUMENT COLLECTION
LIBRARY LOAN COPY
DO NOT TRANSFER TO ANOTHER PERSON
If you wish someone else to see this document, send in name with document and the library will arrange a loan.
UCN-7969
(3 3-67)

NOTICE This document contains information of a preliminary nature and was prepared primarily for internal use at the Oak Ridge National Laboratory. It is subject to revision or correction and therefore does not represent a final report.

LEGAL NOTICE

This report was prepared as an account of Government sponsored work. Neither the United States, nor the Commission, nor any person acting on behalf of the Commission:

A. Makes any warranty or representation, expressed or implied, with respect to the accuracy, completeness, or usefulness of the information contained in this report, or that the use of any information, apparatus, method, or process disclosed in this report may not infringe privately owned rights; or

B. Assumes any liabilities with respect to the use of, or for damages resulting from the use of any information, apparatus, method, or process disclosed in this report.

As used in the above, "person acting on behalf of the Commission" includes any employee or contractor of the Commission, or employee of such contractor, to the extent that such employee or contractor of the Commission, or employee of such contractor prepares, disseminates, or provides access to, any information pursuant to his employment or contract with the Commission, or his employment with such contractor.

ORNL-TM-2263

Contract No. W-7405-eng-26

METALS AND CERAMICS DIVISION

PHYSICAL AND MECHANICAL PROPERTIES OF TYPE 406 STAINLESS STEEL

H. E. McCoy, Jr.

OCTOBER 1968

OAK RIDGE NATIONAL LABORATORY
Oak Ridge, Tennessee
operated by
UNION CARBIDE CORPORATION
for the
U.S. ATOMIC ENERGY COMMISSION

LOCKHEED MARTIN ENERGY RESEARCH LIBRARIES

3 4456 0513079 2

CONTENTS

	Page
Abstract	1
Introduction	1
Experimental Details	2
Material	2
Tensile and Creep-Rupture Tests	3
Oxidation Tests	4
Thermal Expansion Measurements	5
Experimental Results	5
Annealing Studies	5
Tensile and Creep-Rupture Experiments	8
Oxidation Studies	27
Thermal Expansion Measurements	33
Welding Studies	35
Summary	35
Acknowledgments	38

PHYSICAL AND MECHANICAL PROPERTIES OF TYPE 406 STAINLESS STEEL

H. E. McCoy, Jr.

ABSTRACT

Several of the mechanical and physical properties of type 406 stainless steel were evaluated. The tensile properties were determined over the range 25 to 982°C and the creep-rupture properties were determined at 704, 816, and 927°C. Oxidation tests were run in air and flowing CO_2 over the temperature range 816 to 1371°C. The oxidation rates in air and CO_2 were equivalent. The thermal expansion was measured from 25 to 982°C. Structural changes during annealing and welding were noted.

INTRODUCTION

Several types of nuclear reactors require structural materials with good oxidation resistance at elevated temperatures. The oxidizing environment may be steam, air, or some gas such as CO_2 or impure helium. The other requirements vary from system to system, but it is generally desired that the structural material have a low cross section for neutron capture and good mechanical strength at the service temperature.

One class of materials that meets most requirements is the iron-chromium-aluminum alloys. These alloys are ferritic and their primary shortcoming is their low high-temperature strength. Another problem is an embrittlement of the material by the formation of the intermetallic Fe_3Al (ref. 1) at aluminum contents higher than 5%. For optimum oxidation resistance the chromium content should be at least 12% (ref. 2). However, the formation of brittle sigma phase (iron, chromium) becomes a

---

[1]S. L. Case and K. R. Van Horn, p. 310 in Aluminum in Iron and Steel, Wiley, New York, 1953.

[2]Ibid., p. 302.

problem if the chromium content exceeds about 17% (ref. 3). The commercial alloy, type 406 stainless steel, satisfies these requirements with a nominal composition of 12 to 14% Cr and 3.5 to 4.5 Al (ref. 4).

Type 406 stainless steel has received little attention as a structural material. The primary reason for its development seems to have been for use as a heating element material.[4] This fact alone attests to the alloy's good oxidation resistance. Pessl[5] included this alloy in a comparative evaluation of several alloys for use in high-temperature CO_2 and water systems. Jones[6] also discussed this alloy in an interpretive literature survey concerning the oxidation characteristics of several alloys. The general conclusion was that the alloy has very good oxidation resistance and this was supported by data by Pessl in steam and CO_2 environments. However, the data do not exist concerning the physical and mechanical properties of this alloy that are necessary for evaluating its suitability for an engineering system.

Because of the interest in gas-cooled reactors at ORNL, a brief study was undertaken to determine more of the mechanical and physical properties of type 406 stainless steel. This study included annealing experiments, tensile and creep-rupture tests, oxidation tests in air and CO_2, thermal expansion measurements, and cursory welding investigations.

EXPERIMENTAL DETAILS

Material

This alloy is not usually stocked by steel producers and it was necessary to purchase an entire heat of material. The heat was produced

---

[3]J. J. Heger, The Formation of Sigma Phase in 17 Per Cent Chromium Steel, "Symposium on the Nature, Occurrence, and Effects of Sigma Phase," Am. Soc. Testing Mater. Spec. Tech. Publ. 110, 75 (1951).

[4]Metals Handbook, 1948 ed. (ed. by T. Lyman) American Society for Metals, Cleveland, Ohio, 1948, p. 555.

[5]H. J. Pessl, Evaluation of Iron- and Nickel-Base Alloys for Medium and High Temperature Reactor Applications, Part I, HW-67715 (February 1961).

[6]D. A. Jones, Gas-Metal Reactions with Iron- and Nickel-Base Heat Resistant Alloys, HW-76952 (March 1963).

by The Carpenter Steel Company and the 350-lb yield was delivered as 1-in.-diam rods. The as-received material had been annealed at an undesignated temperature. These rods were cold swaged to 3/4 in. before test specimens were made. The chemical analysis of the material is given in Table 1.

Table 1. Chemical Analysis of Test Material

Element	Content, wt %	
	Vendor	ORNL
Cr	14.08	14.1
Al	3.91	3.91
Ni		0.44
Mn	0.43	0.41
Si	0.41	0.35
Ti		0.32
Zr		0.11
C	0.08	0.079, 0.090
O		0.0038
N		0.019
P	0.016	
S	0.013	

Tensile and Creep-Rupture Tests

The geometry of the test specimen used in the tensile and creep-rupture tests is shown in Fig. 1. The tensile tests were run in a 12,000-lb Baldwin Hydraulic testing machine at a strain rate of 0.02 min^{-1}. These tests were run in an air environment. The creep-rupture tests in air were run in standard creep machines. The tests in argon utilized a chamber with sliding U-cup seals at both ends. The specimen was heated to the test temperature under vacuum for degassing purposes. The chamber was purged with argon to a pressure of 10 psig and isolated from the gas supply for the test. Strips of zirconium getter were attached near the specimen to help maintain the purity of the test environment. Temperatures were measured with Chromel-P–Alumel thermocouples (accuracy = ±3/4%) and controlled with L and N proportioning potentiometric control units (control accuracy = ±1/4%). The

ORNL-DWG 63-6434
ALL DIMENSIONS ARE IN INCHES

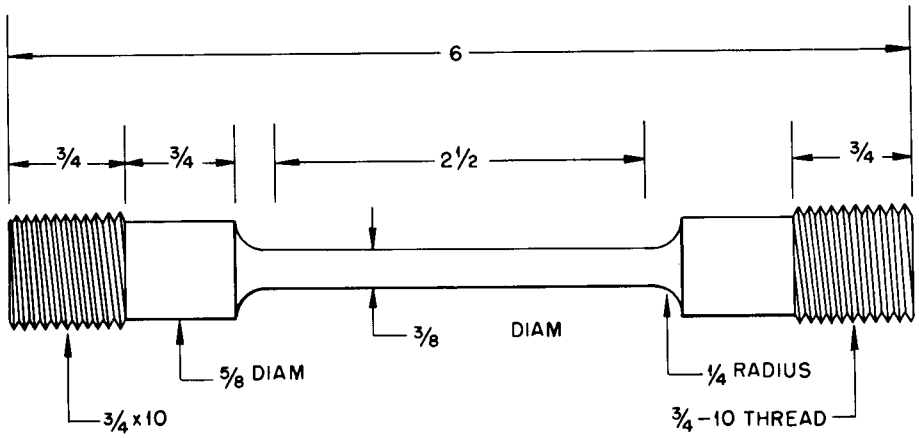

Fig. 1. Test Specimen for Tensile and Creep-Rupture Studies.

temperature was initially quite uniform along the specimen; however, the very high elongations encountered made it difficult to maintain the entire gage length at a uniform temperature. Hence, the actual strains may be even larger than those measured.

Oxidation Tests

The gravimetric technique was used for measuring the rate of oxidation. Two specific types of equipment were utilized. One type was an Ainsworth automatic recording balance, where the change in the weight of the specimen was recorded as a function of time. The second type utilized a steel wire spring with a quartz fiber that extended into the furnace to support the specimen. The springs were calibrated so that the change in length could be correlated with a change in the specimen weight.

Both types of apparatus were sealed so that the test environment could be controlled. The equipment was first evacuated and then purged with either CO_2 or air. When the furnace had reached the desired temperature, the specimen was lowered into place and rate measurements were initiated. The CO_2 was passed over CuO at 400°C to oxidize any CO to CO_2 and over Drierite for removing moisture. The air test environment was obtained by using compressed plant air after drying. Both test gases were circulated at a rate of 0.1 scfh.

Thermal Expansion Measurements

These measurements were made in a quartz dilatometer. The apparatus utilized a specimen 0.250 in. in diameter by 2 in. long. The dial indicator that was used to measure the change in length was enclosed in a bell jar so that the entire system could be run in vacuum. The thermocouple (Pt–10% Rh vs Pt) was attached to the outside of the quartz tube (approx 0.010 in. from specimen). The specimen was heated and cooled at a linear rate of 1°C/min.

EXPERIMENTAL RESULTS

Annealing Studies

This alloy should be completely ferritic at all temperatures and should not be amenable to heat treatments involving transformation to austenite or martensite.[7] The material for these experiments was cold swaged from 1 to 0.75 in. in diameter, a reduction in area of 44%. Complete recrystallization was obtained by annealing for 1 hr at 816°C, the lowest temperature investigated. The microstructure after this treatment is shown in Fig. 2. The very fine dots in Fig. 2(a) appear to be etch pits, although their formation may be enhanced by the presence of fine Al_2O_3 precipitates. Several large inclusions are present and numerous large precipitates [marked by arrow in Fig. 2(b)] that have the gold-color characteristic of Ti-C-N compounds. We examined these precipitates with the electron microprobe analyzer and found that the precipitates were titanium base with the concentration of aluminum being $< 0.1\%$. The same type of microstructure was obtained by annealing 1 hr at 982°C (Fig. 3). However, annealing for 1 hr at 1093°C caused appreciable grain growth to occur (Fig. 4). Based on these experiments, we chose a pretest heat treatment of 1 hr at 982°C.

---

[7] D. S. Clark and W. R. Varney, p. 318 in Physical Metallurgy for Engineers, Van Nostrand, Princeton, New Jersey, 1962.

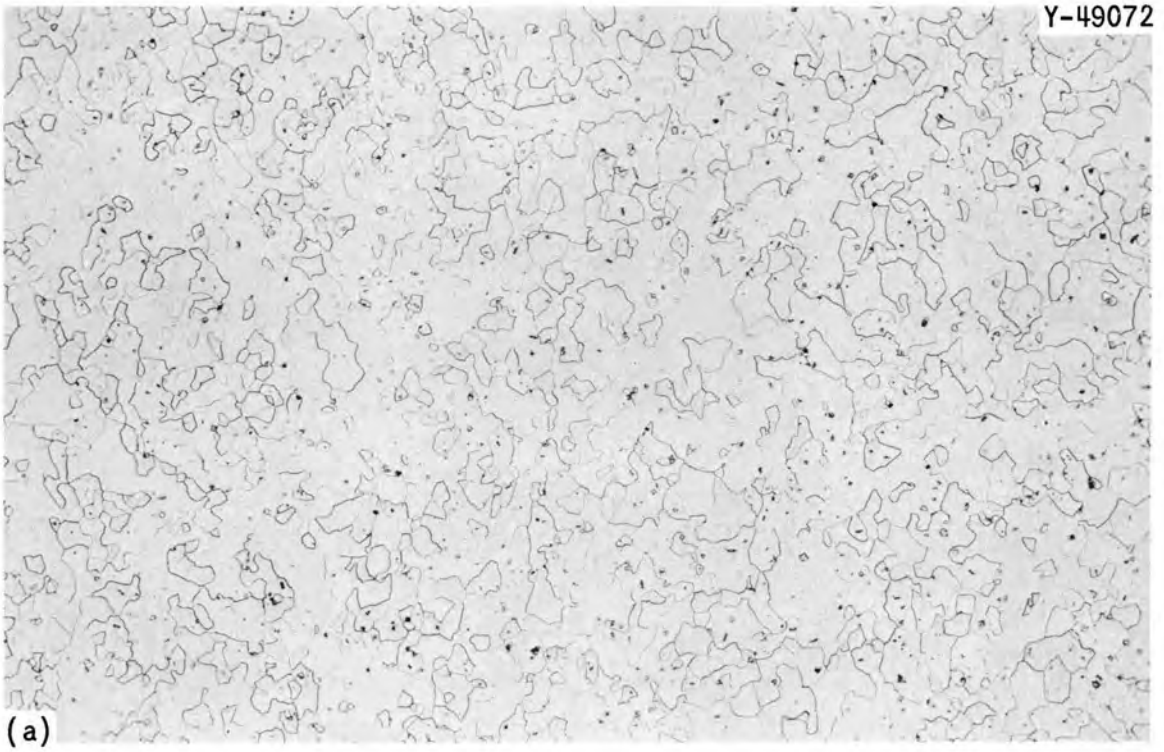

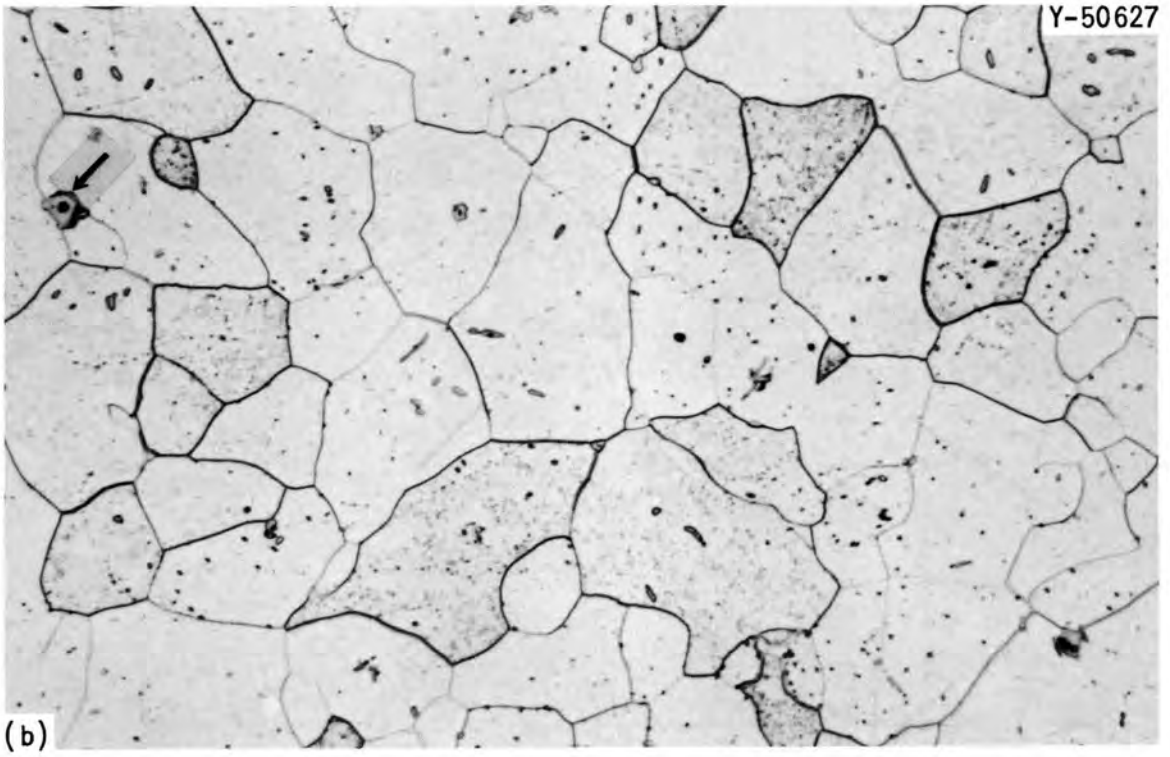

Fig. 2. Typical Microstructure After Annealing 1 hr at 816°C. (a) 100×. (b) 500×. Etchant: glyceria regia.

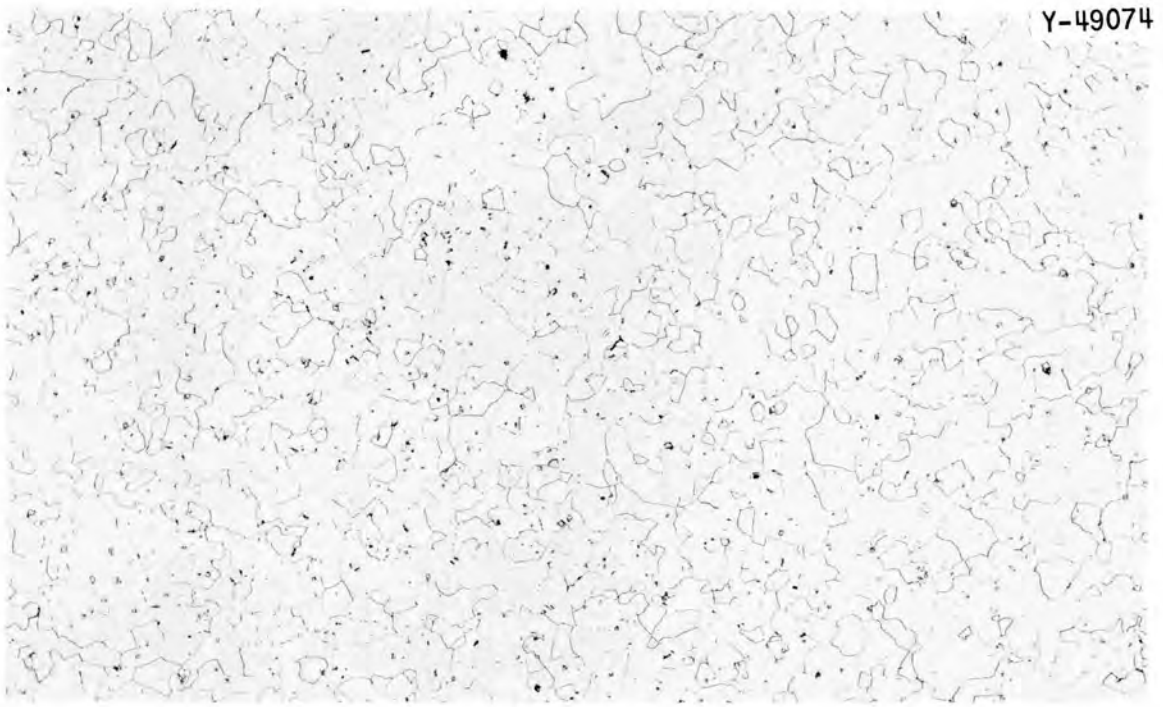

Fig. 3. Typical Microstructure After Annealing 1 hr at 982°C. 100×. Etchant: glyceria regia.

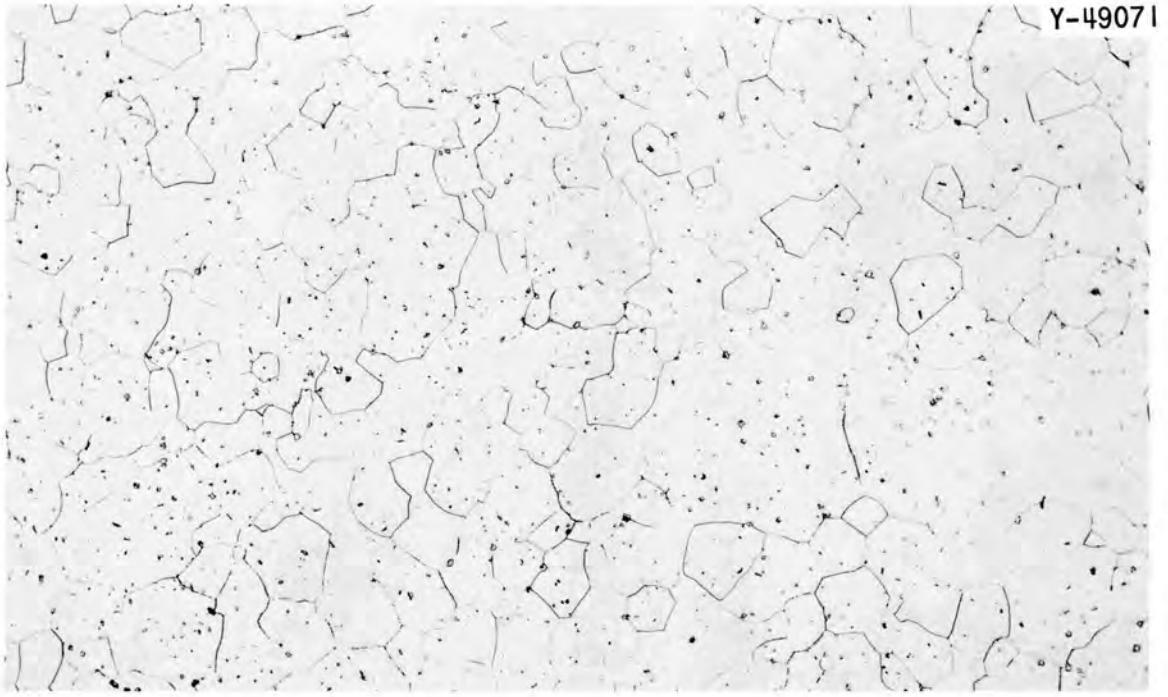

Fig. 4. Typical Microstructure After Annealing 1 hr at 1093°C. 100×. Etchant: glyceria regia.

Tensile and Creep-Rupture Experiments

Several tensile tests were run in the temperature range of 25 to 927°C. The yield and ultimate stresses over this temperature range are plotted in Fig. 5 and the data are compared in Table 2 with those for type 304 stainless steel (an austenitic steel). At temperatures up to about 500°C, type 406 stainless steel (a ferretic steel) is stronger than the austenitic steel. Above 500°C the strength of the ferretic steel decreases rapidly and the austenitic steel is stronger. Above 700°C the ferritic steel has almost no ability to strain-harden and the yield and ultimate stresses are nearly equivalent. These data also demonstrate the high ductility of the ferritic steel.

Creep-rupture tests were run at 704, 816, and 927°C in both air and argon environments. The results of the tests are summarized in Tables 3, 4, and 5. The creep-rupture properties at 704°C are shown in Fig. 6.

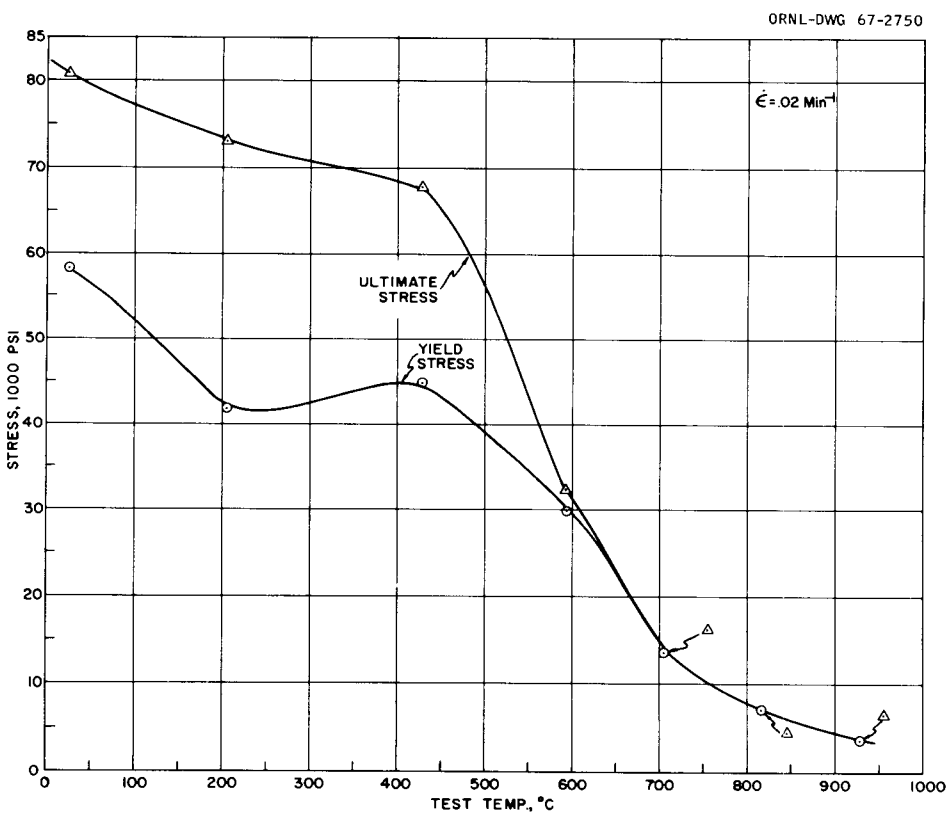

Fig. 5. Tensile Properties of Type 406 Stainless Steel.

Table 2. Comparative Tensile Properties of Types 406 and 304 Stainless Steel

Test Temperature (°C)	Type 406 Stainless Steel[a]				Type 304 Stainless Steel[b]			
	Yield Stress (psi)	Tensile Stress (psi)	Elongation (%)	Reduction in Area (%)	Yield Stress (psi)	Tensile Stress (psi)	Elongation (%)	Reduction in Area (%)
25	58,300	80,800	34.0	68.5	34,000	85,000	63	76
150					23,000	73,000	60	75
204	41,700	73,000	30.0	69.8				
370					16,500	66,000	50	72
427	44,900	67,700	30.0	69.4				
593	29,800	32,300	40.5	86.5	13,000	49,000	40	62
704	13,500	13,500	106.0	97.4	11,000	35,500	37	51
816	7,070	7,070	88.0	98.6	10,000	21,000	39	45
927	3,550	3,550	147.0	99.6		12,000	46	50

[a]Strain rate, 0.02 min^{-1}, annealed 1 hr at 982°C prior to testing.

[b]Steels for Elevated Temperature Service, U.S. Steel, 1949, p. 60.

Table 3. Creep-Rupture Results at 704°C

Test Number	Stress (psi)	Environment	Rupture Life (hr)	Elongation at Rupture (%)	Reduction in Area (%)	Minimum Creep Rate (%/hr)	Time to Indicated Strain, hr			
							1%	2%	5%	10%
2458	12,000	Argon	0.20	67.5	95.2					
2486	7,000	Argon	4.1	80.0	95.9	3.99	0.25	0.50	1.28	2.3
2548	4,500	Argon	43.0[a]	45.3	46.9	0.328	2.9	6.2	13.9	22.0
3214	4,500	Argon	33.9	78.8	93.7	0.340	2.9	5.6	12.2	19.7
2769	4,500	Air	26.1	40.4	93.7	0.556	0.7	2.2	7.7	14.0
2538	3,000	Argon	307.0[a]	42.5	51.0	0.0313	42	74	143	205
3217	3,000	Argon	305.0	77.8	97.2	0.020	48	84	151	209
3080	3,000	Air	362.4	112.0	93.7	0.035	22	50	111	175
3355	3,000	Air	313.9	121.7	97.2	0.028	30	61.5	119.5	175
3215	2,000	Argon	2756.8	80.3	94.0	0.00065	1010	1325	1780	2140
3076	2,000	Air	3002.8	66.3	93.7	0.00074	1120	1480	1910	2250

[a]Test discontinued during tertiary creep slightly prior to fracture.

Table 4. Creep-Rupture Results at 816°C

Test Number	Stress (psi)	Environment	Rupture Life (hr)	Elongation at Rupture (%)	Reduction in Area (%)	Minimum Creep Rate (%/hr)	Time to Indicated Strain, hr			
							1%	2%	5%	10%
3081	3000	Air	5.1	130	100	3.39	0.28	0.57	1.3	2.17
3220	2000	Air	34.5	100	99.3	0.160	4.5	7.9	14.2	19.8
3236	1300	Argon	233.6	93.4	81.3	0.0193	41	59	90.5	123
3218	1300	Air	279.8	56.1	88.9	0.0114	54	80	126	175
3417	900	Argon	774.4	76.3	74.1	0.0040	112	175	290	415
3226	900	Argon	798.9[a]	80.4	61.0	0.0052	110	175	270	392
3386	900	Air	868.5	80.0	74.0	0.0025	152	202	306	434
3937	700	Argon	1861.8	77.5	73.8	0.0011	255	350	590	935

[a]Test discontinued during tertiary creep slightly prior to fracture.

Table 5. Creep-Rupture Results at 927°C

Test Number	Stress (psi)	Environment	Rupture Life (hr)	Elongation at Rupture (%)	Reduction in Area (%)	Minimum Creep Rate (%/hr)	Time to Indicated Strain, hr			
							1%	2%	5%	10%
2460	2000	Argon	1.5	76.2	100	7.8	0.075	0.20	0.46	0.74
2477	1000	Air	27.0[a]	158.7	86.4	0.32	2.6	4.2	7.9	13
3219	700	Argon	129.5[a]	86.3	70.4	0.103	7.7	14.8	34.0	60.2
2567	500	Argon	465.9	84.6	76.6	0.0495	20	37	92	190
4043	500	Air	486.3	81.3	82.2	0.055	13	27	73	170
3216	400	Argon	1270.1	82.7	87.0	0.018	27	61	199	470
3079	300	Argon	3149.2	84.0	87.0	0.0071	60	145	530	1200
2570	300	Air	2170.6	100.7	82.4	0.0069	60	130	495	1030

[a]Test discontinued during tertiary creep slightly prior to fracture.

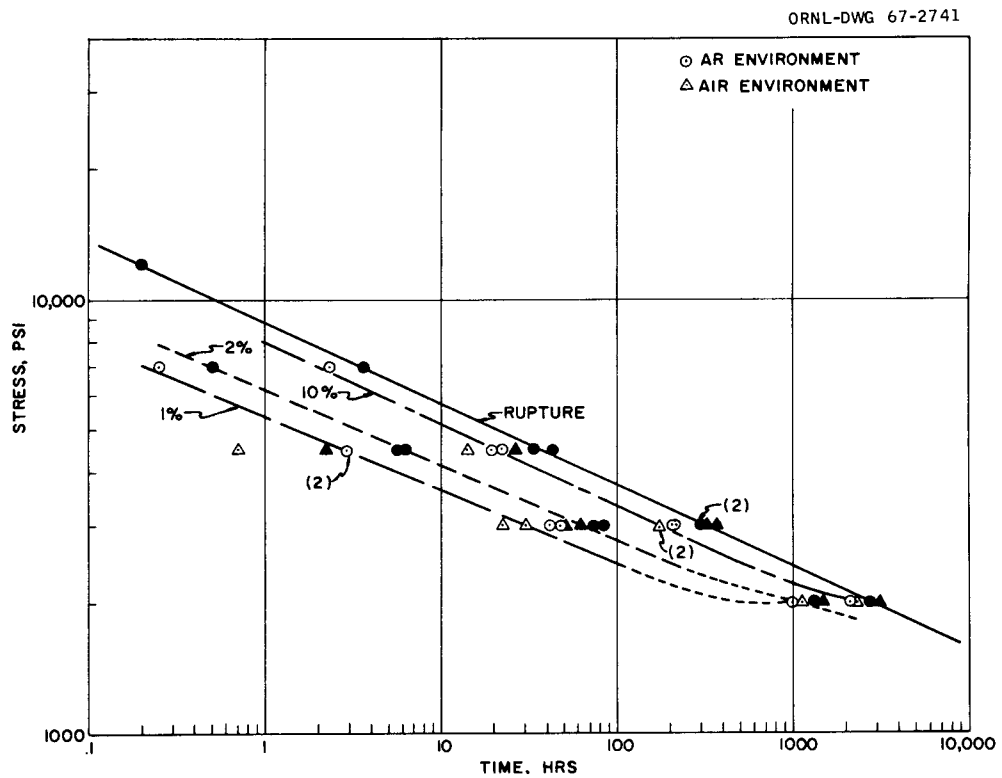

Fig. 6. Creep-Rupture Properties of Type 406 Stainless Steel at 704°C.

The time-to-rupture correlates well with stress on logarithmic coordinates, but the time to reach low strains shows some deviation at low-stress levels. The minimum creep rate and stress are plotted in Fig. 7 and some deviation from linearity is noted.

The creep-rupture results at 816°C are shown in Fig. 8. The data can not be described on logarithmic coordinates by a straight line. A better correlation is obtained by plotting linear stress versus the logarithm of the time (Fig. 9). The logarithm of the minimum creep rate and linear stress are also related by a straight line (Fig. 10).

At 927°C the creep-rupture results again are linear when plotted on logarithmic coordinates (Fig. 11). The minimum creep rate and the stress are also linear on logarithmic coordinates (Fig. 12).

None of the results indicate an appreciable influence of the air or argon test environment. The specimens tested in both environments were discolored after testing, although those tested in air were oxidized more heavily. An effect might be noted if a test specimen with a larger ratio of surface area to volume were used.

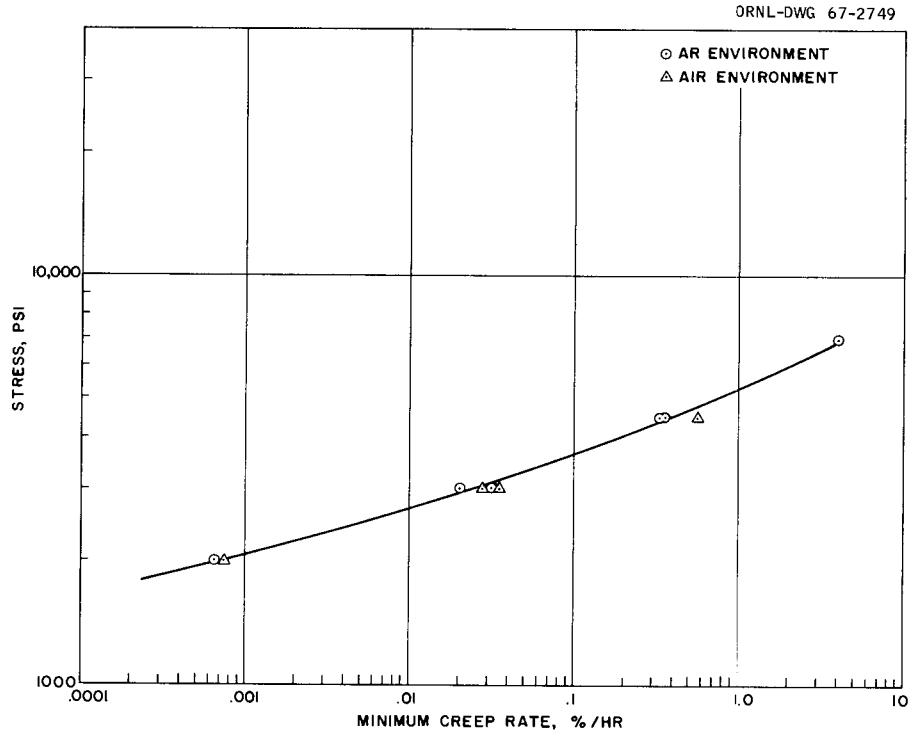

Fig. 7. Relation of Stress and Minimum Creep Rate for Type 406 Stainless Steel at 704°C.

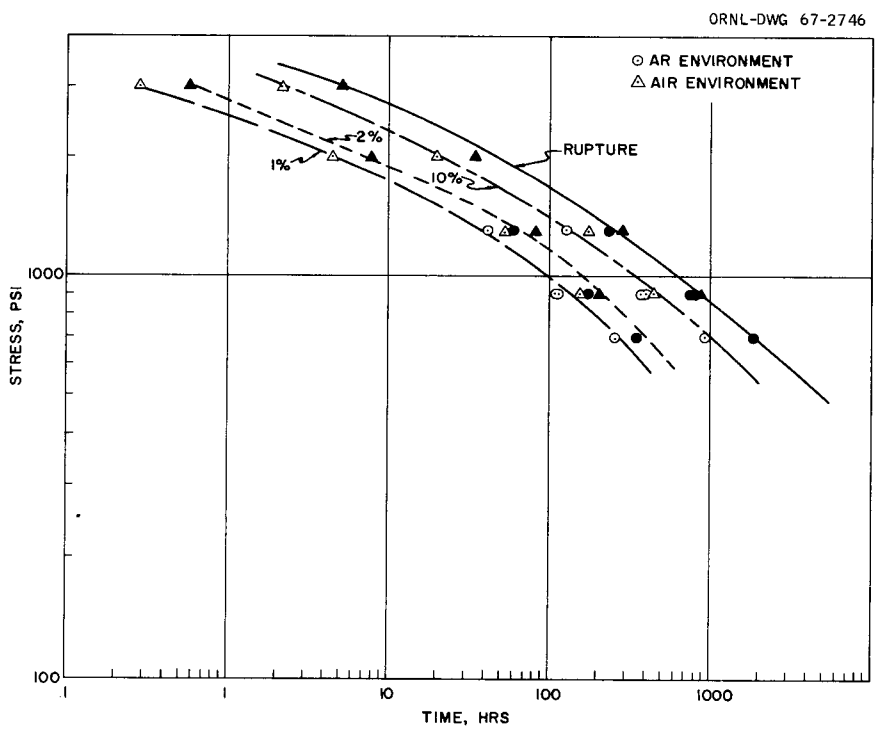

Fig. 8. Creep-Rupture Properties of Type 406 Stainless Steel at 816°C on Logarithmic Coordinates.

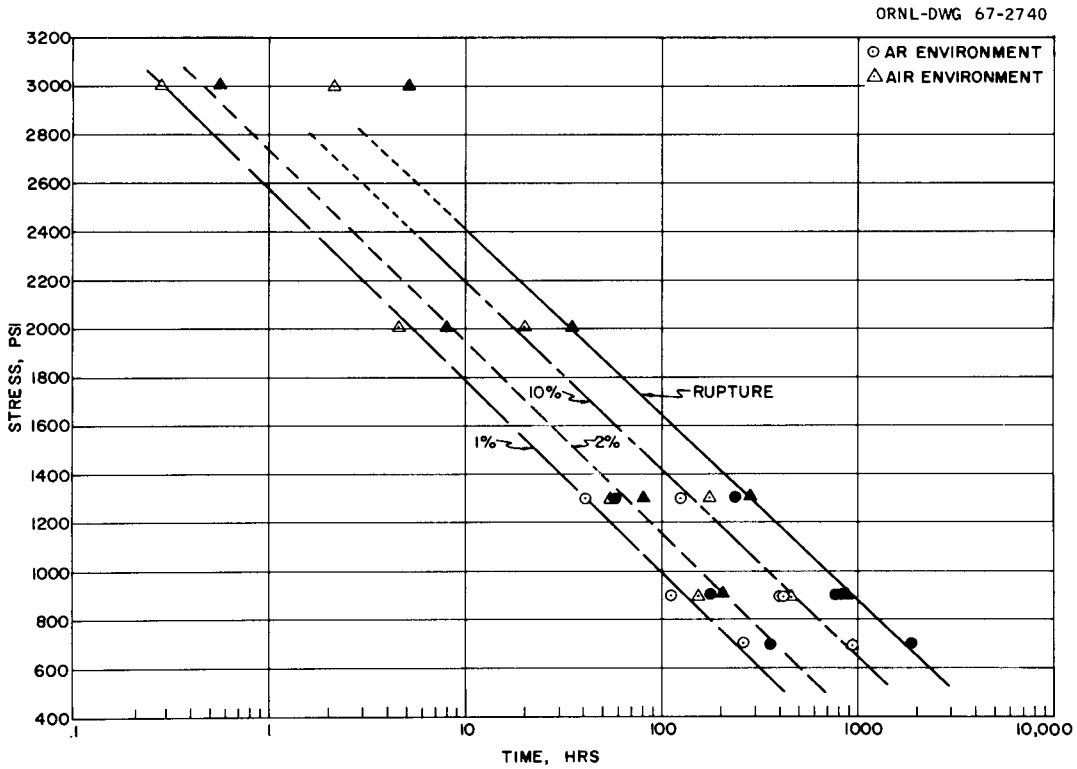

Fig. 9. Creep-Rupture Properties of Type 406 Stainless Steel at 816°C.

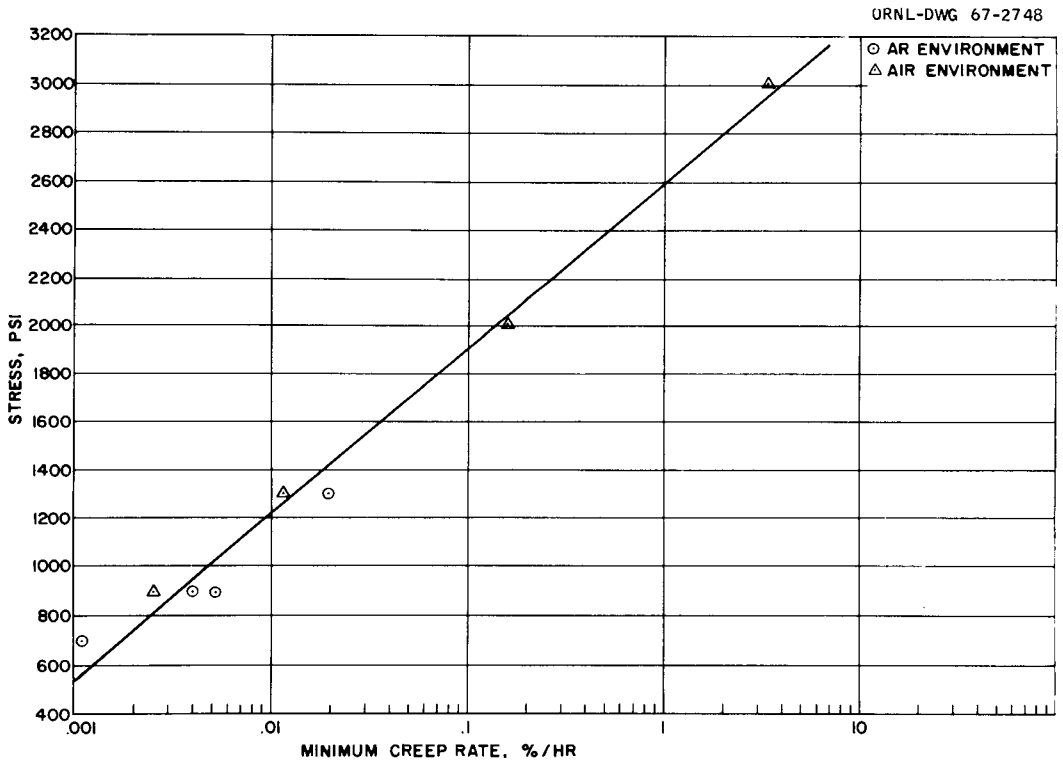

Fig. 10. Relation of Stress and Minimum Creep Rate for Type 406 Stainless Steel at 816°C.

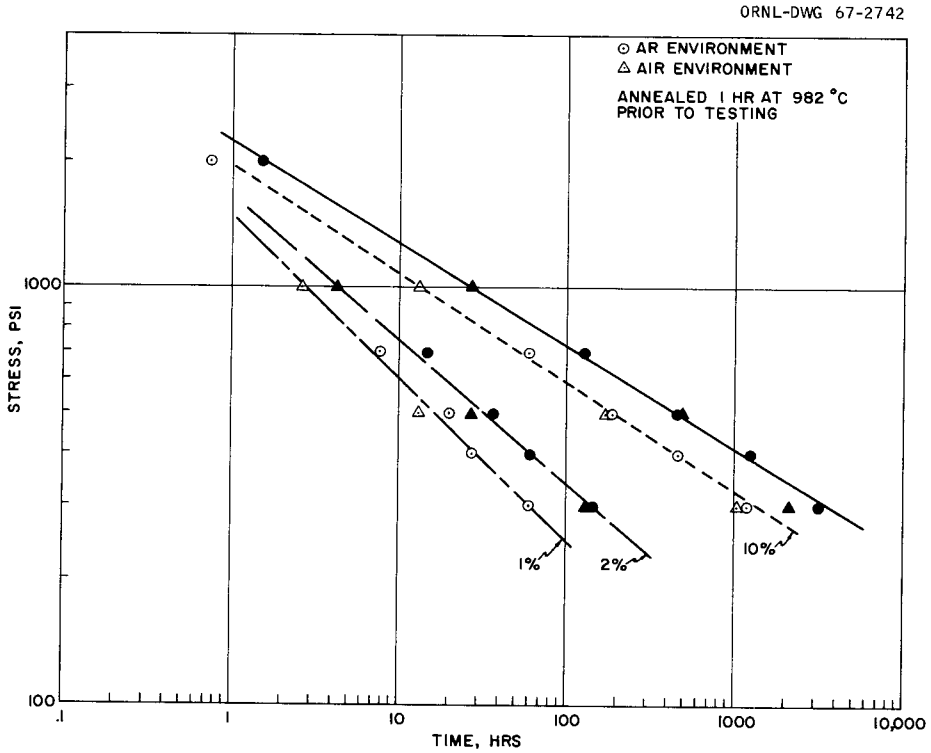

Fig. 11. Creep-Rupture Properties of Type 406 Stainless Steel at 927°C.

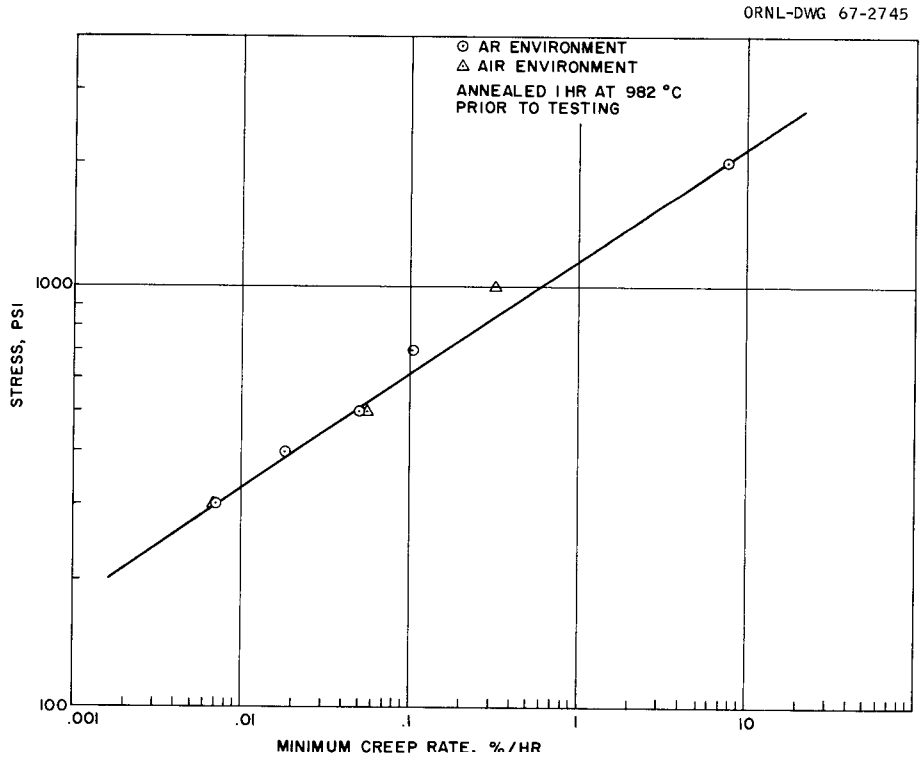

Fig. 12. Relation of Stress and Minimum Creep Rate for Type 406 Stainless Steel at 927°C.

Another correlation of the test results is shown in Fig. 13. Machlin[8] predicted from theoretical considerations that the product of strain rate and the time to rupture should be a constant (independent of stress and temperature) when creep is controlled by vacancy condensation. Monkman and Grant[9] and McCoy[10] have shown that this general relationship holds for several materials but that often the strain rate must be considered to a power slightly different from unity. For type 406 stainless

[8]E. S. Machlin, "Creep-Rupture by Vacancy Condensation," Trans. Met. Soc. AIME 206, 106 (1956).

[9]F. C. Monkman and N. J. Grant, "An Empirical Relationship Between Rupture Life and Minimum Creep Rate in Creep-Rupture Tests," Am. Soc. Testing Mater. Proc. 56, 593 (1956).

[10]H. E. McCoy, Effects of Hydrogen on the High-Temperature Flow and Fracture Characteristics of Metals, ORNL-3600 (June 1964).

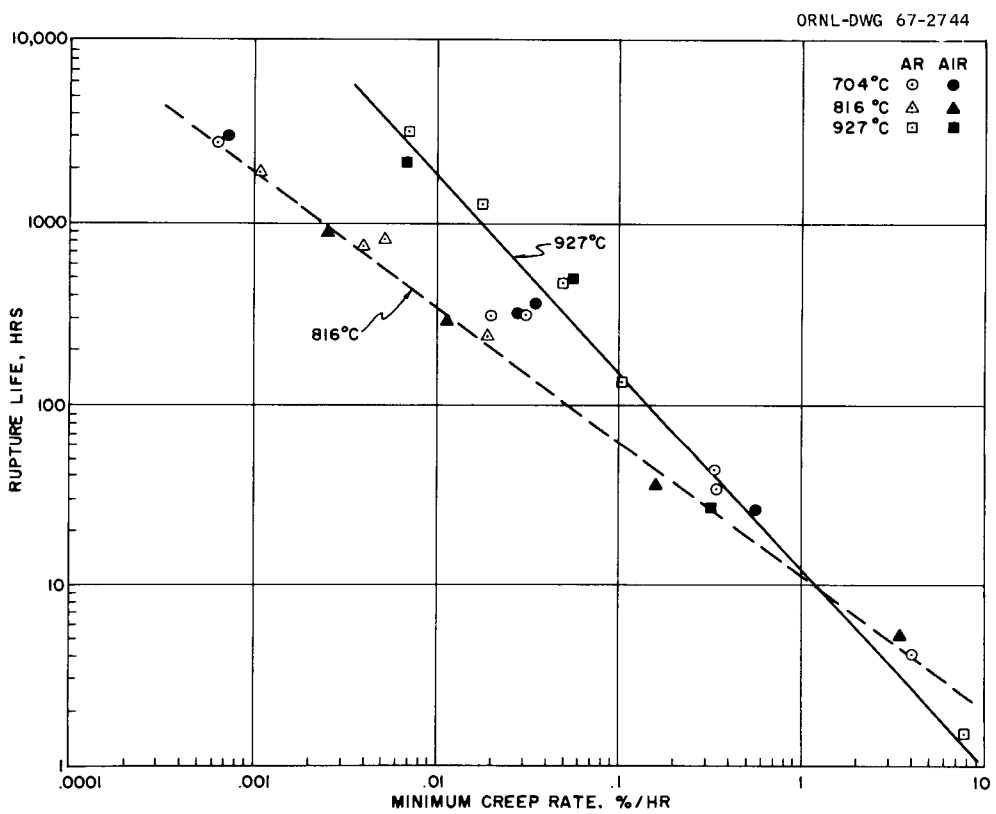

Fig. 13. Relation of Rupture Life and Minimum Creep Rate for Type 406 Stainless Steel.

steel at 927°C (Fig. 13) the data correlate well with a slope of about −1. At 816°C the slope is about −0.75, but a good correlation is still obtained. At 704°C the data are not described adequately by a straight line.

The data obtained at the three temperatures were correlated by the Larson-Miller parameter.[11] Plots for the times to 1, 2, 5, and 10% strain and rupture are shown in Figs. 14, 15, 16, 17, and 18, respectively. The respective values for the constant used in computing the parameter and for the constants describing the equation of each curve are given in Table 6. The extension of the line to the left in each plot should not be used, since the stress levels predicted are too high.

The fracture strains were very high under all test conditions with most values between 75 and 90%. The reduction in area measurements exhibited less scatter and all values were between 70 and 100%. As shown in Fig. 19, the reduction in area was not affected appreciably by test temperature and decreased slightly with increasing rupture life.

Several of the specimens were examined metallographically after testing. Figure 20(a) shows the fracture of a specimen tested at 704°C. The grains appear to be heavily deformed. There are numerous elongated voids and the fracture has been largely due to the linking of these voids with the final separation being transgranular. Figure 20(b) shows the microstructure about 1/2 in. from the fracture. The grains are elongated and numerous voids (mostly intergranular) are evident. Figure 20(c) shows that many of the voids originate from cracks within or at the interface of the precipitates.

The fracture of a specimen tested at 816°C is shown in Fig. 21(a). The main features are similar to those observed in material tested at 704°C (Fig. 20); however, at 816°C the individual grains are not worked as heavily and the intergranular voids are larger and more rounded. Figure 21(b) shows the structure about 1/2 in. away from the fracture.

---

[11] F. R. Larson and James Miller, "A Time-Temperature Relationship for Rupture and Creep Stresses," Trans. ASME (Am. Soc. Mech. Engrs.) 74, 765 (1952).

ORNL-DWG 66-12915

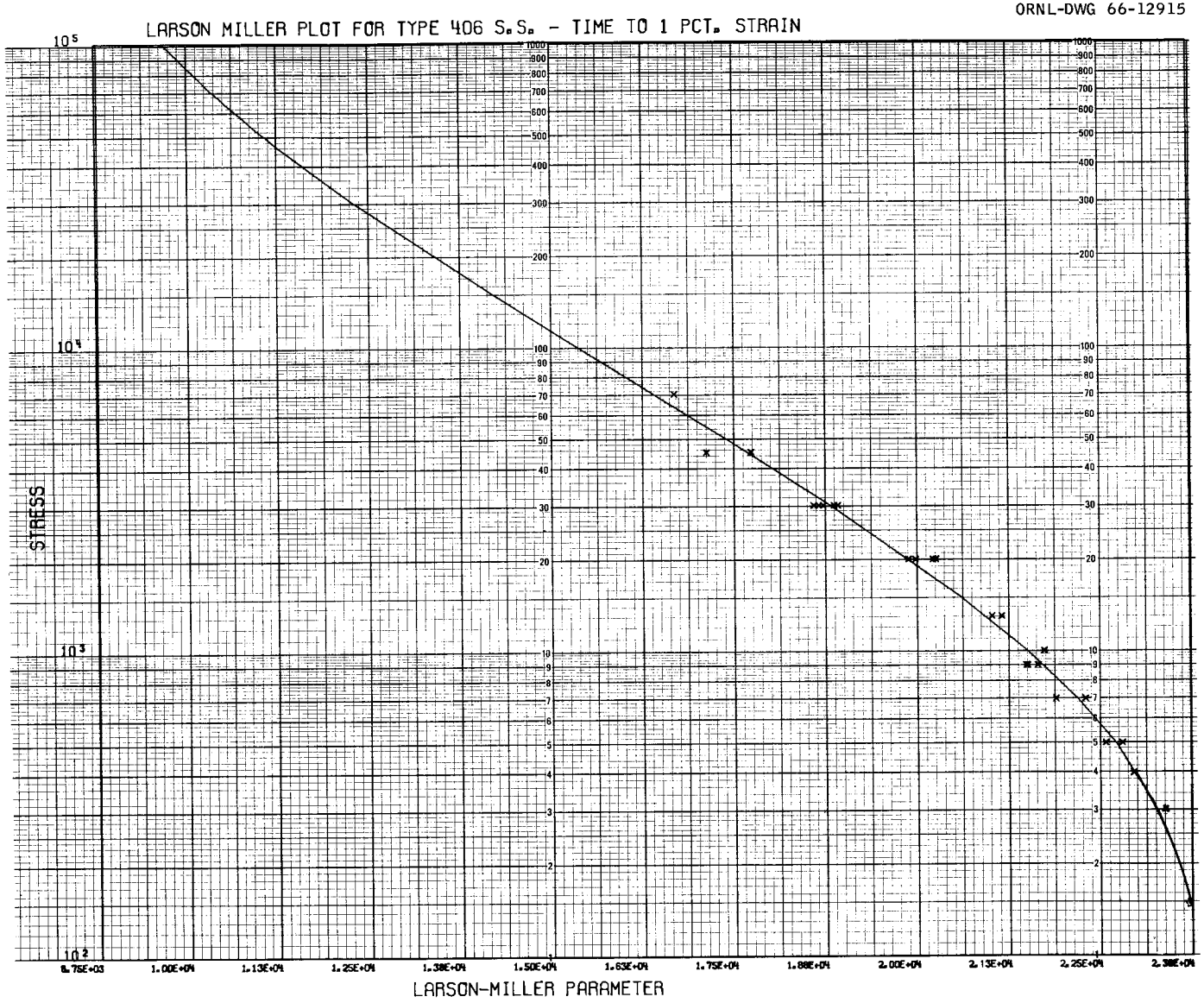

Fig. 14. Larson-Miller Plot for Type 406 Stainless Steel — Time to 1% Strain.

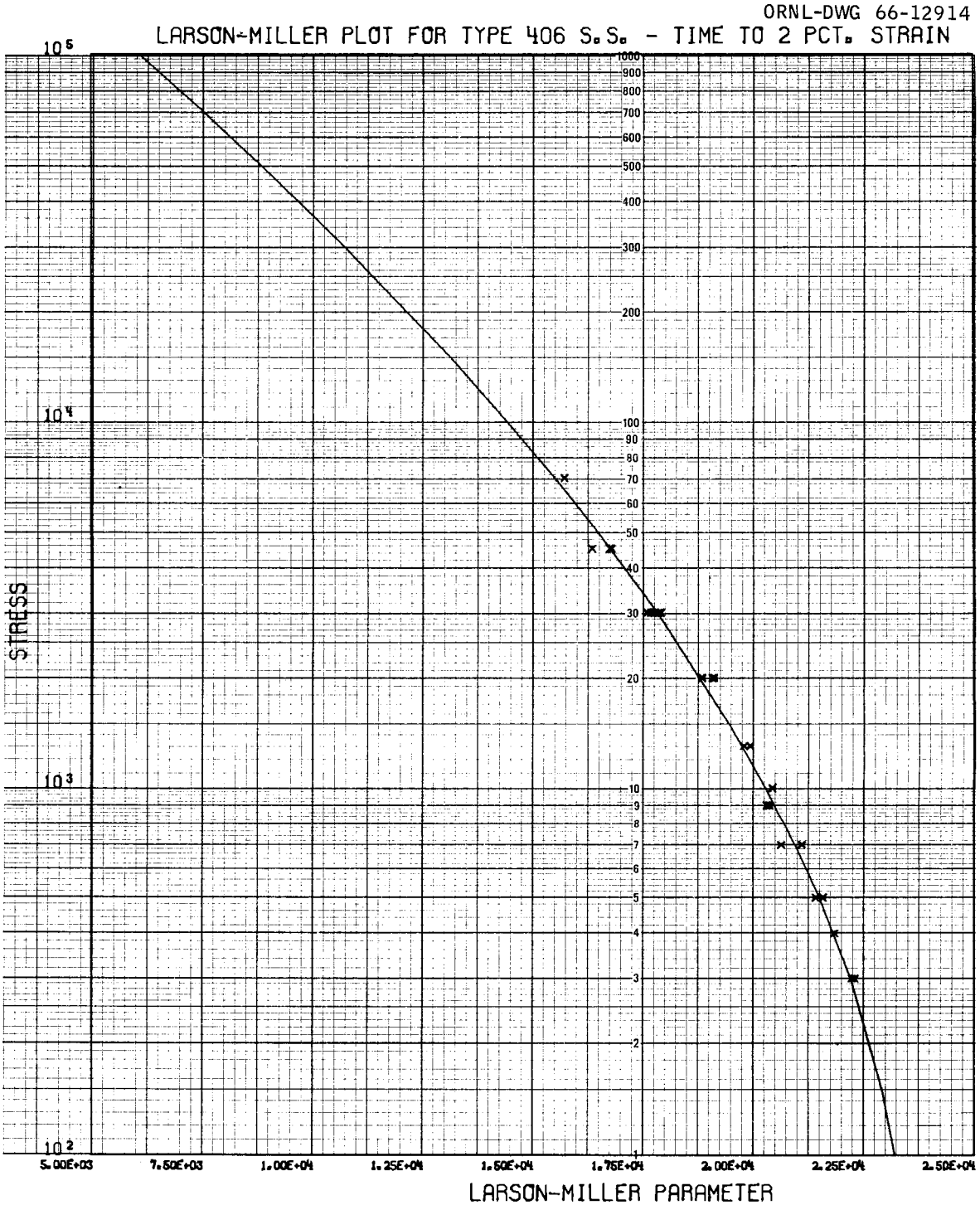

Fig. 15. Larson-Miller Plot for Type 406 Stainless Steel — Time to 2% Strain.

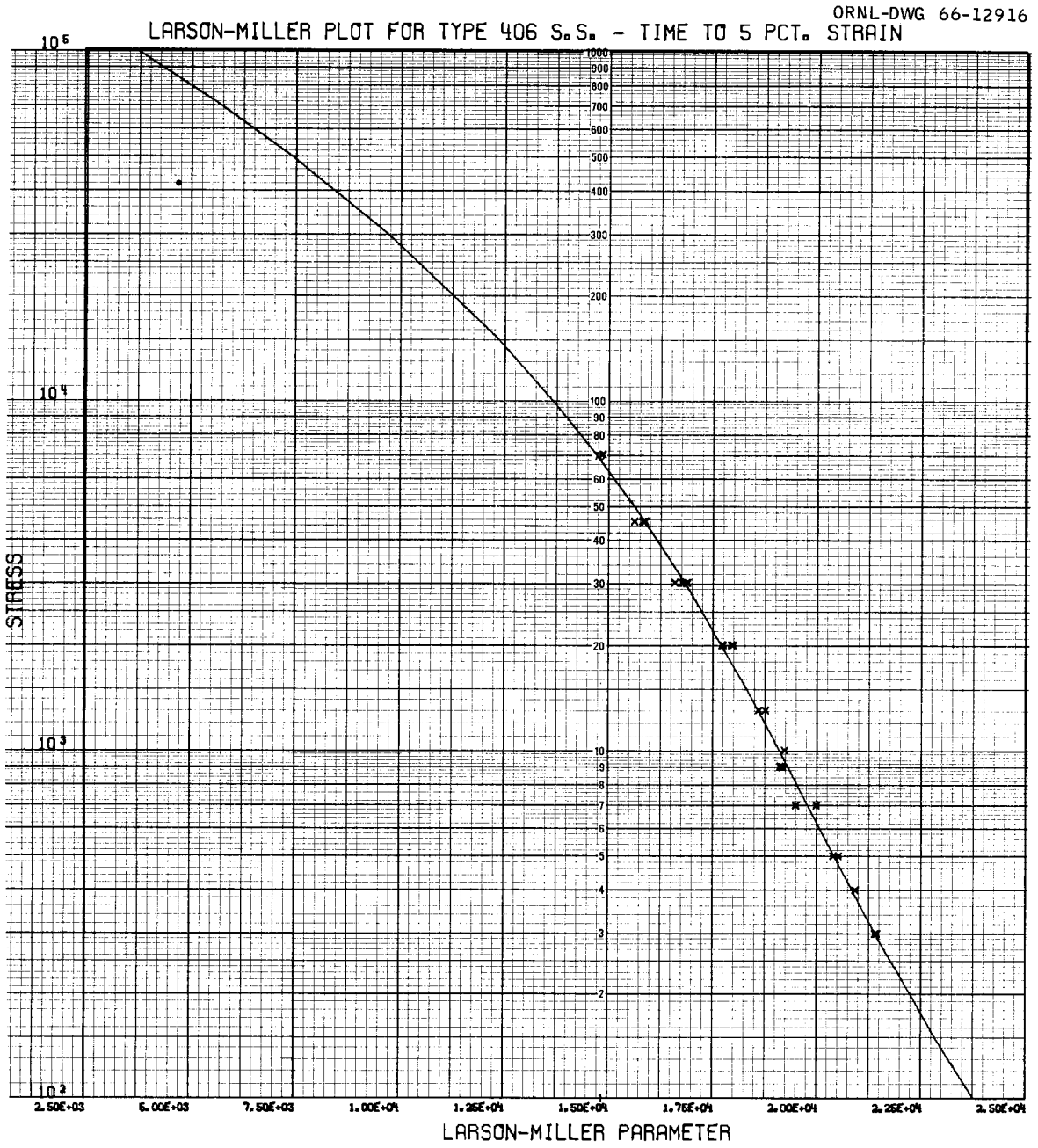

Fig. 16. Larson-Miller Plot for Type 406 Stainless Steel — Time to 5% Strain.

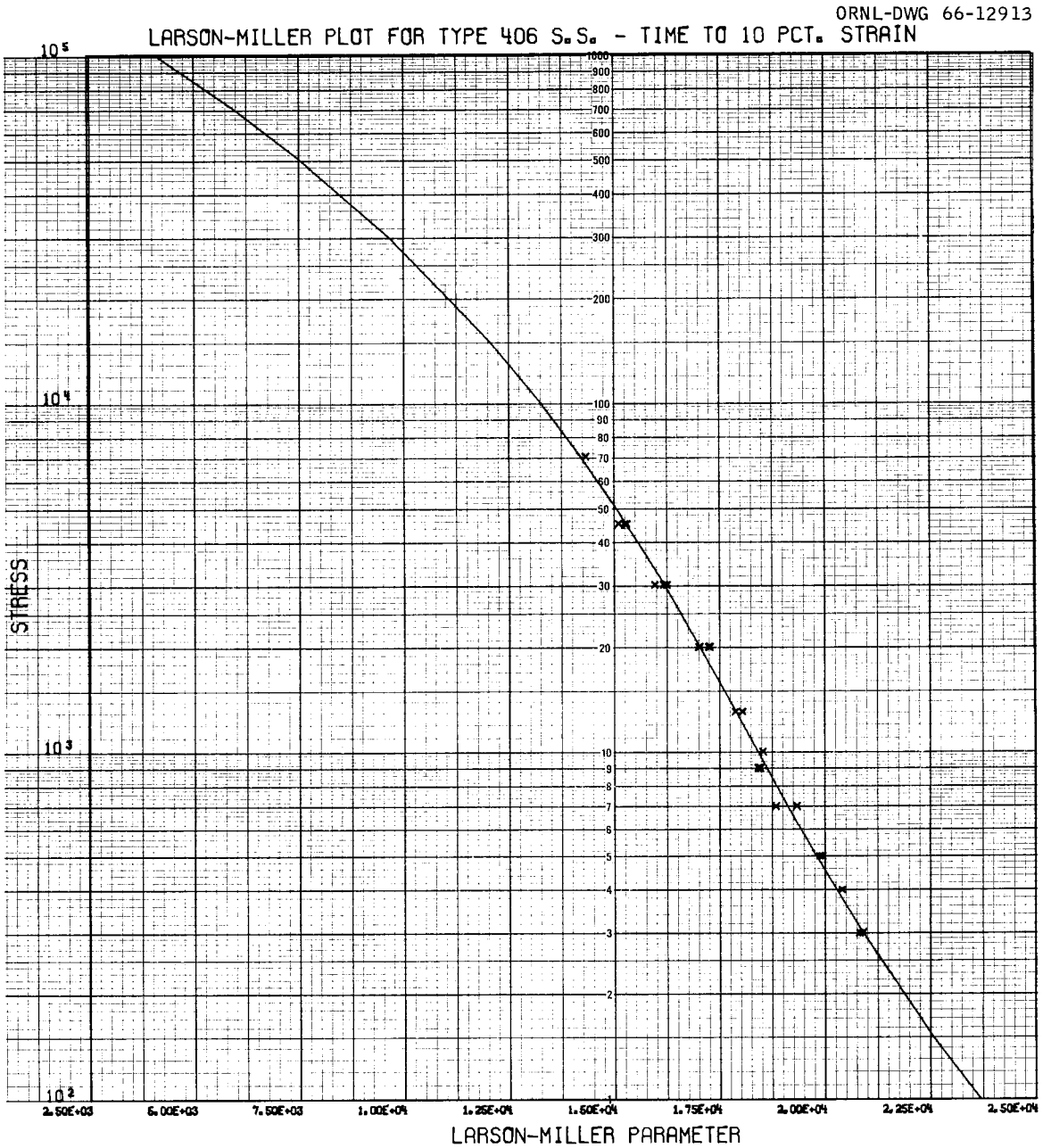

Fig. 17. Larson-Miller Plot for Type 406 Stainless Steel — Time to 10% Strain.

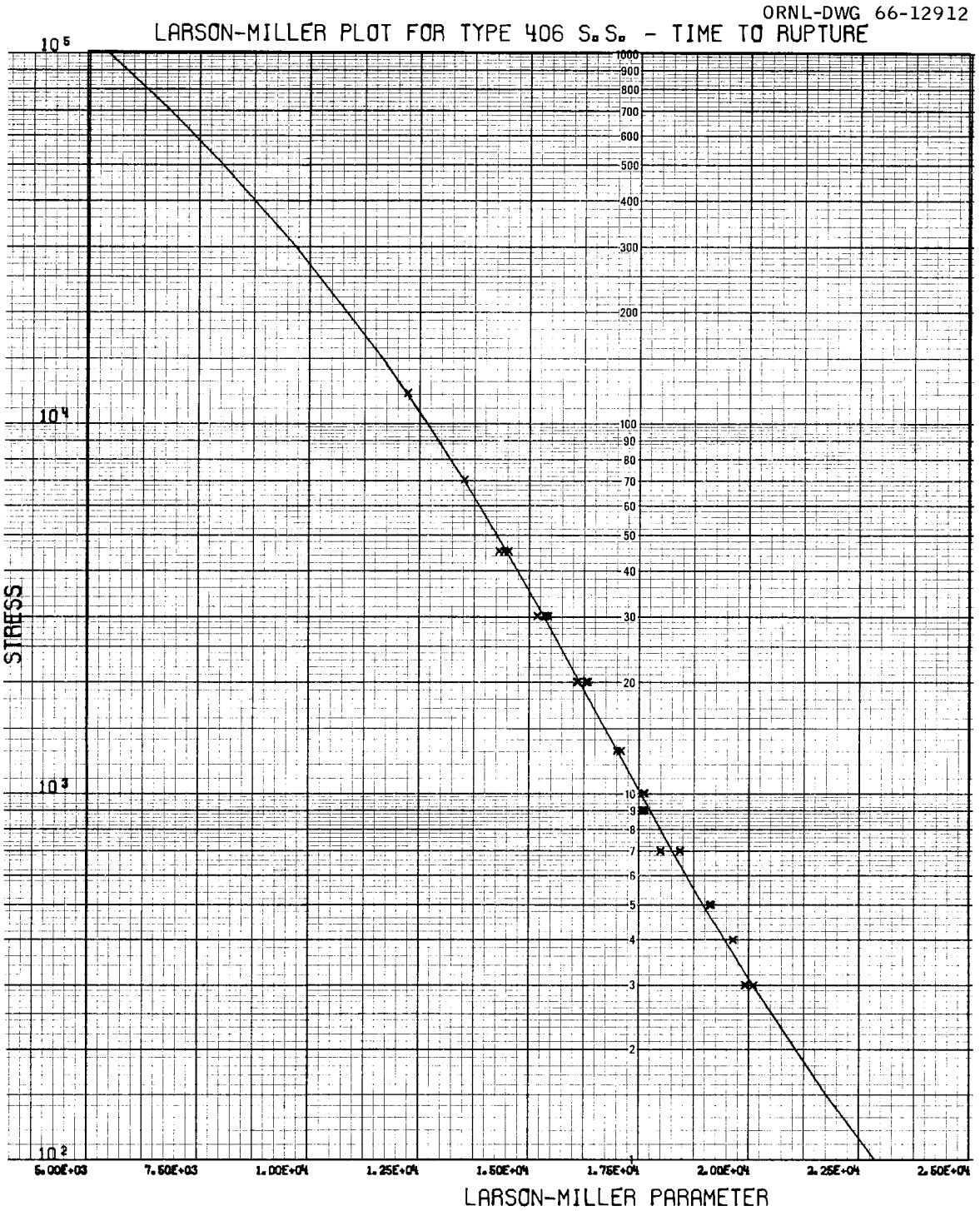

Fig. 18. Larson-Miller Plot for Type 406 Stainless Steel — Time to Rupture.

Table 6. Constants[a] for Larson-Miller Plots

Plot	Constants				
	C	A_o	A_1	A_2	A_3
1% strain	17.7	-5.85×10^3	3.03×10^4	-9.47×10^3	8.07×10^2
2% strain	16.4	1.84×10^4	6.42×10^3	-2.15×10^3	7.55×10^1
5% strain	15.1	4.59×10^4	1.92×10^4	5.30×10^3	-6.32×10^2
10% strain	14.3	5.13×10^4	-2.36×10^4	6.31×10^3	-6.94×10^2
Rupture	13.3	4.63×10^4	-1.89×10^4	4.53×10^3	-4.78×10^2

[a]Constants based on the following equations: (1) defining equation of the Larson-Miller parameter, P,

$$P = T(C + \log t) ,$$

(2) cubic equation of the Larson-Miller plot

$$P = A_o + A_1x + A_2x^2 + A_3x^3 ,$$

where

t = time, hr,
T = absolute temperature, °K,
x = log stress.

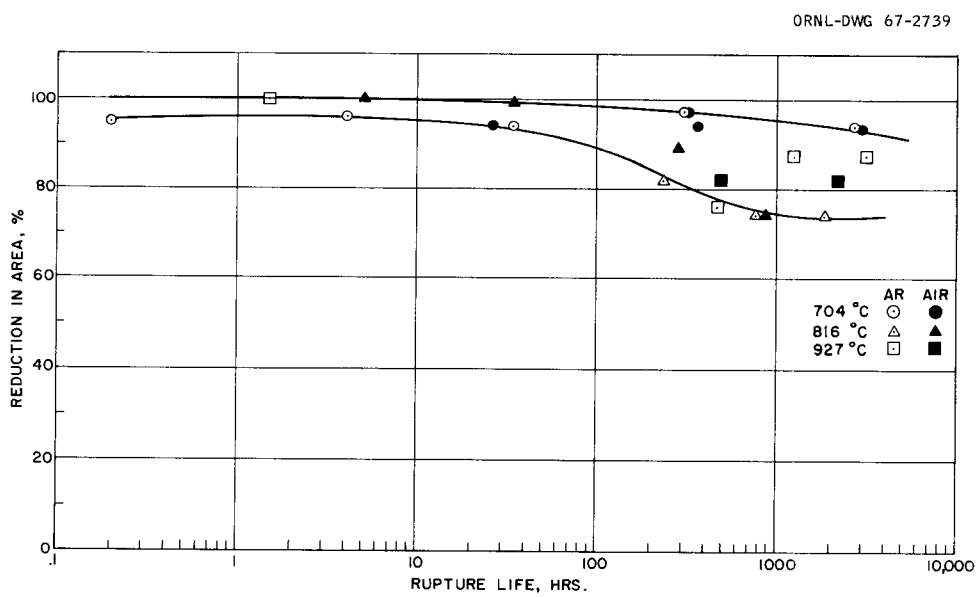

Fig. 19. Variation of Reduction in Area with Rupture Life for Type 406 Stainless Steel.

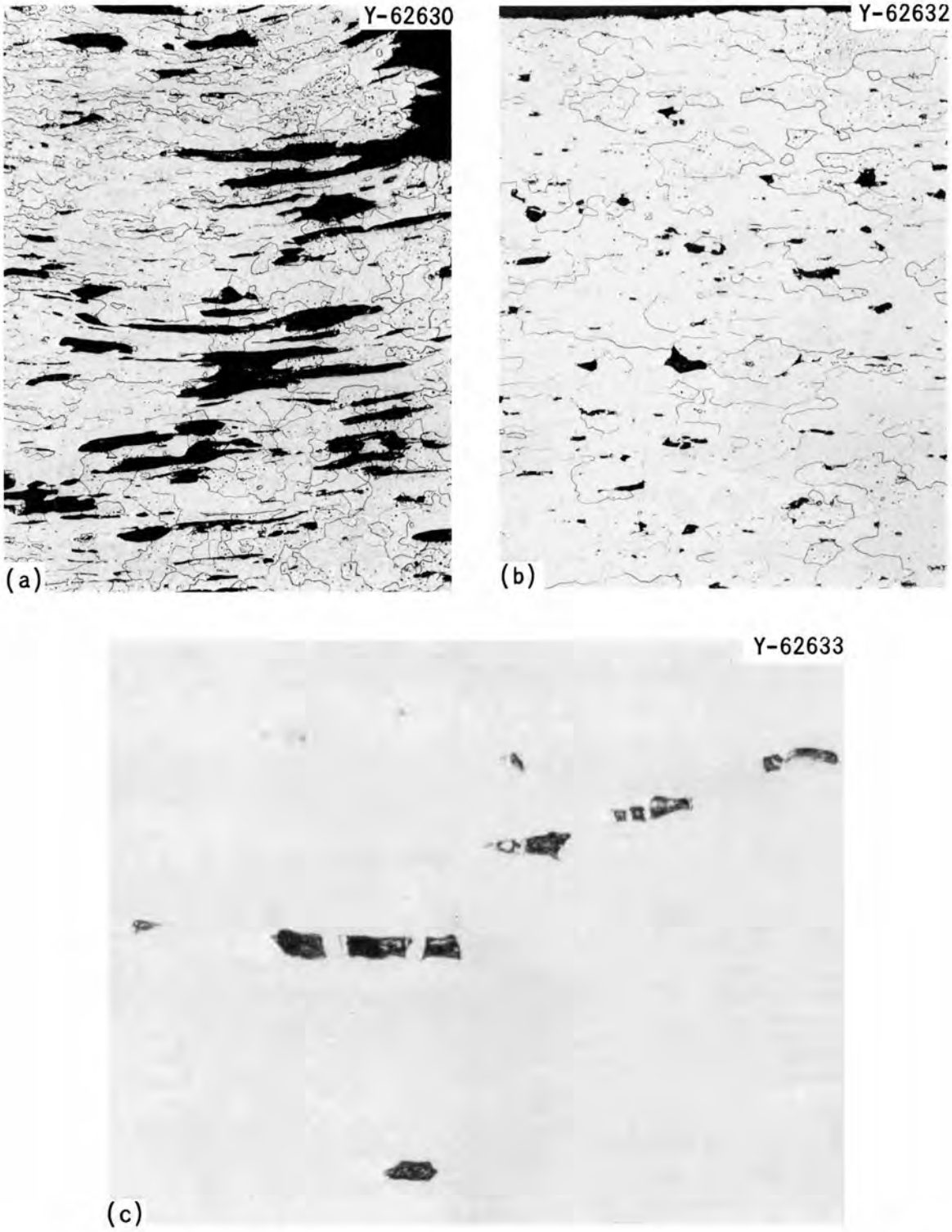

Fig. 20. Microstructures of Specimen Tested at 704°C and 2000 psi in Argon. Specimen failed in 2757 hr with 80% strain. (a) Fracture and (b) 1/2 in. from fracture, 100×. Etchant: glyceria regia. (c) Typical, as polished, 500×.

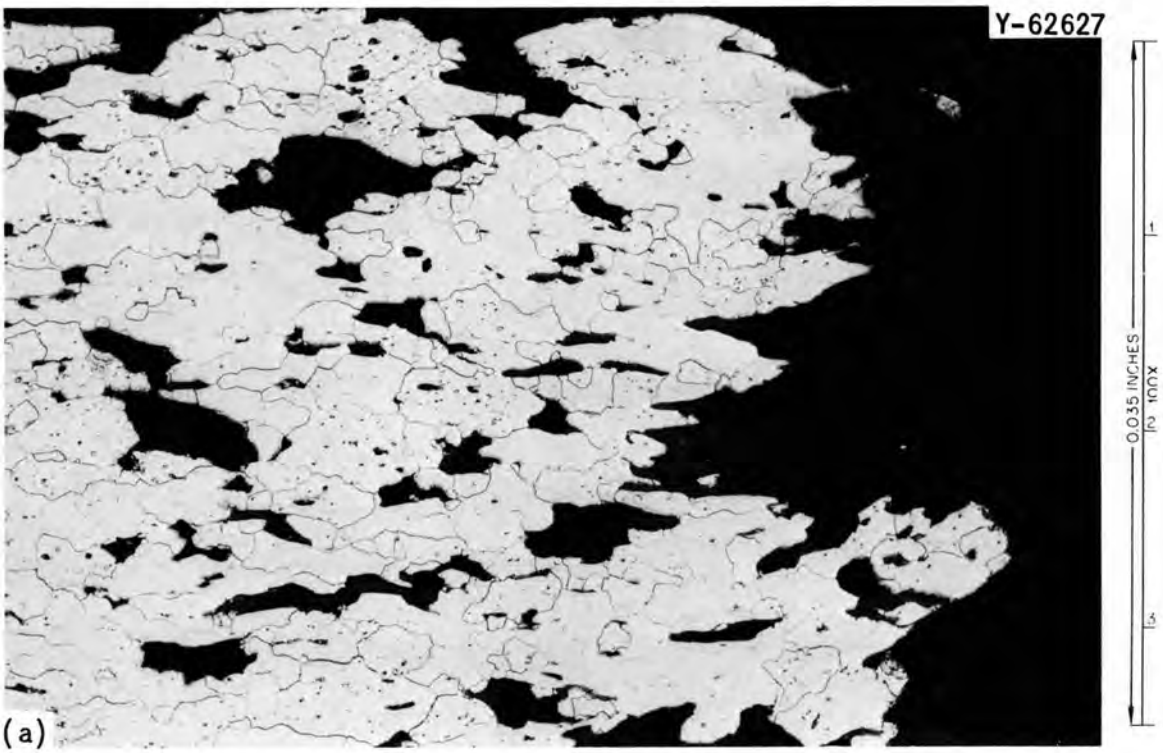

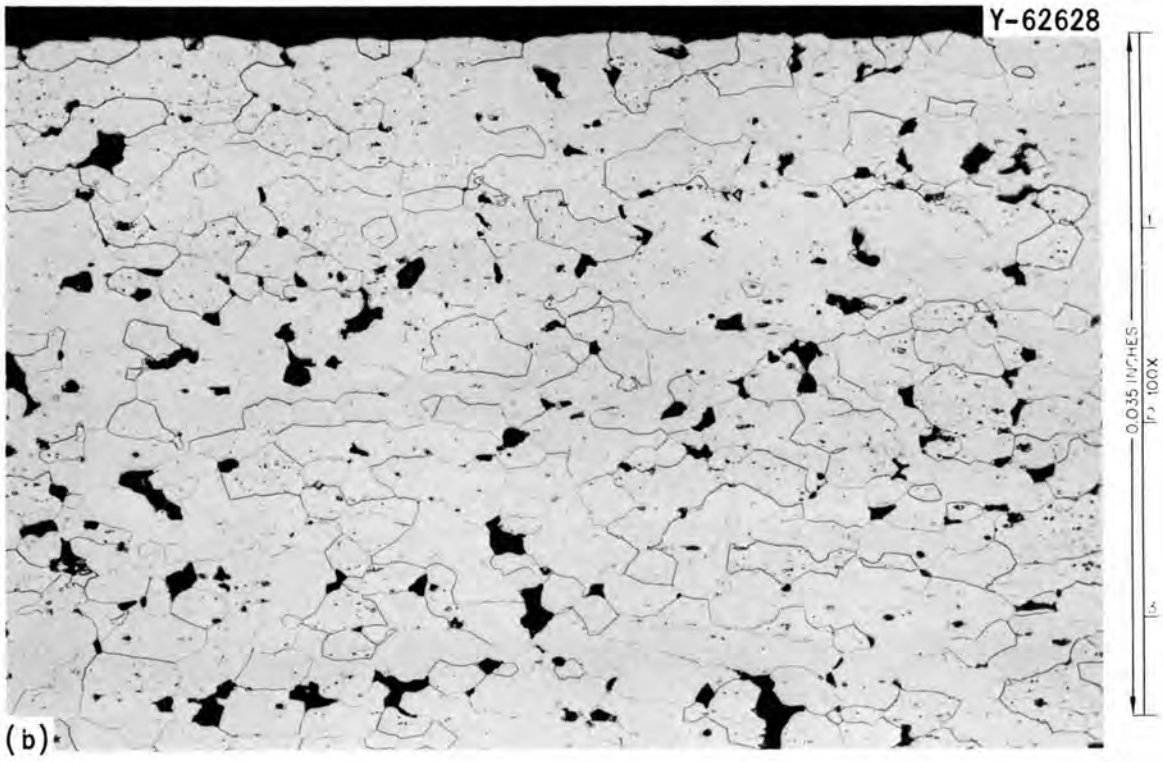

Fig. 21. Photomicrographs of Specimen Tested at 816°C and 900 psi in Air. Failure occurred in 869 hr with 80% strain. (a) Fracture and (b) 1/2 in. from fracture. Etchant: glyceria regia.

A typical fracture of a specimen tested at 927°C is shown in Fig. 22(a). Significant features are evidence of grain growth, largely intergranular fracture, and large intergranular voids. Figure 22(b) shows an area about 1/2 in. from the fracture. Again, significant grain growth has occurred and large intergranular voids have formed.

None of the metallographic studies revealed any differences in specimens tested in argon and air environments. The oxide films formed under all conditions were very thin and adherent and seemed to have no effect on the formation of cracks near the surface.

Oxidation Studies

Slices were cut from the 1-in.-diam rod and rolled to 0.005-in.-thick foil for oxidation studies. The tests run in air are summarized in Table 7 and the rate curves are shown in Fig. 23. The oxidation behavior is described after a few hours at each temperature by the expression

$$\Delta W = Kt^n ,$$

where

ΔW = the weight change per unit area, mg/cm^2,

t = time, hr,

K = rate constant, $mg\ cm^{-2}\ hr^{-n}$,

n = constant.

The constant "n" is approximately equal to 0.5 for this material (Table 7), indicating that the oxide being formed is protective and that the rate of oxidation is decreasing with time. The rate constant, K, is plotted as a function of reciprocal temperature in Fig. 24. The rate constant is related to temperature by the Arrhenius equation for a rate process,

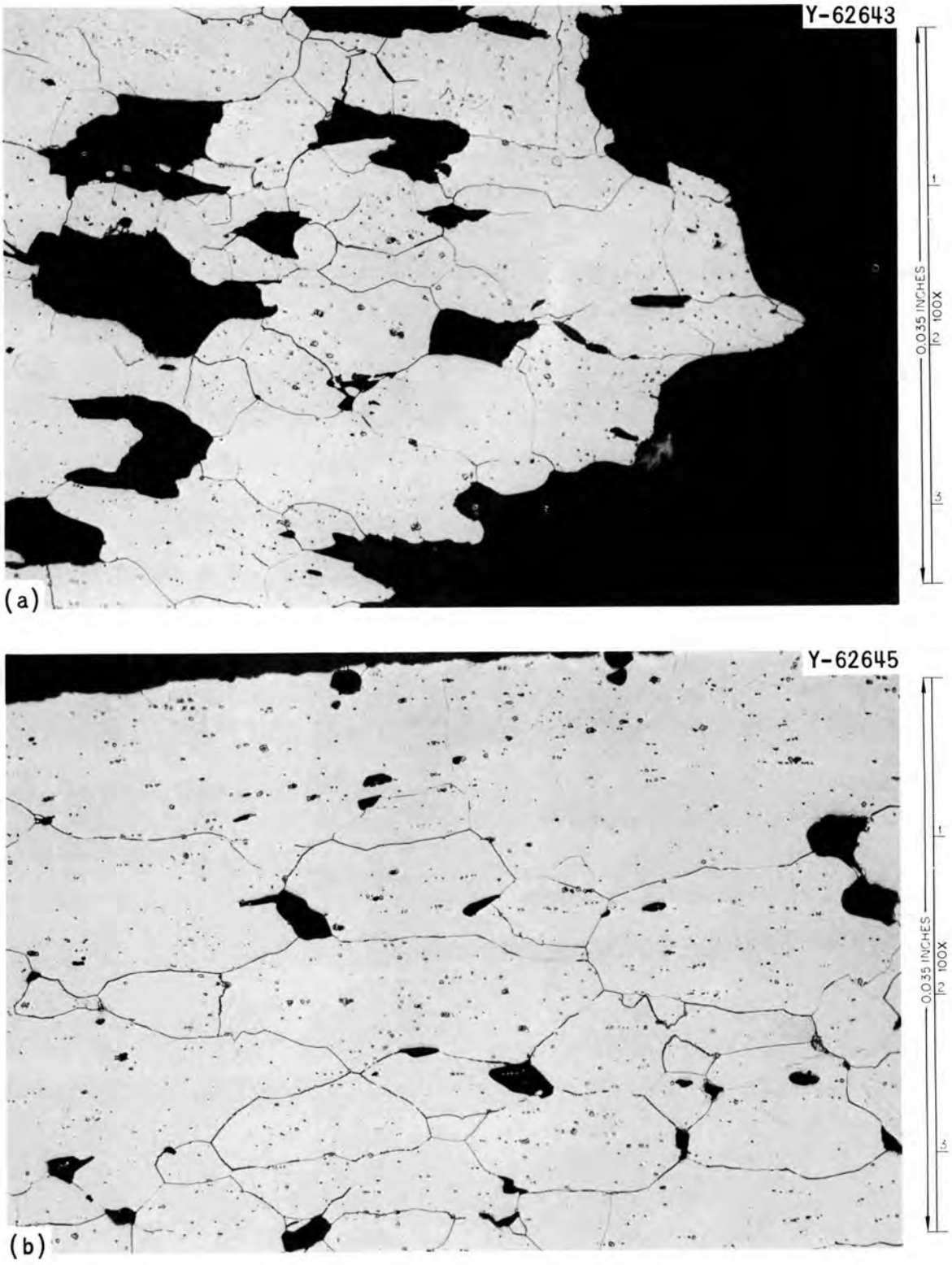

Fig. 22. Photomicrographs of Specimen Tested at 927°C and 300 psi in Air. Failure occurred in 2171 hr with 100% strain. (a) Fracture and (b) 1/2 in. from fracture. Etchant: glyceria regia.

Table 7. Oxidation of Type 406 Stainless Steel in Air

Test Number	Test Temperature (°C)	Exposure Time (hr)	Weight Gain (mg/cm^2)	Time to Beginning of Accelerated Rate (hr)	Weight Gain at Beginning of Accelerated Rate (mg/cm^2)	K[a]	n[a]
3102	816	310	0.147			0.007	0.423
3175	927	408	0.217			0.0202	0.420
3822	927	4541	0.538			0.0190	0.384
3018	982	359	0.381			0.0160	0.522
3210	1038	335	0.848			0.065	0.441
3333	1038	2934	6.32	1070	2.2		
3051	1093	242	1.25			0.091	0.480
3279	1093	594	1.94	480	1.35	0.098	0.430
3252	1149	410	18.6	180	1.5	0.136	0.460
3241	1204	162	18.5	48	1.2	0.250	0.403
3801	1260	66.9	22.1	29	1.1	0.31	0.370
3804	1316	28.3	22.2	9.2	0.88	0.30	0.475
3808	1371	17.0	21.6	5.0	1.0	0.48	0.379

[a]Based on the equation

$$\Delta W = Kt^n ,$$

where

ΔW = weight change per unit area, mg/cm^2,
t = time, hr,
n = constant,
K = rate constant, $mg\ cm^{-2}\ hr^{-n}$.

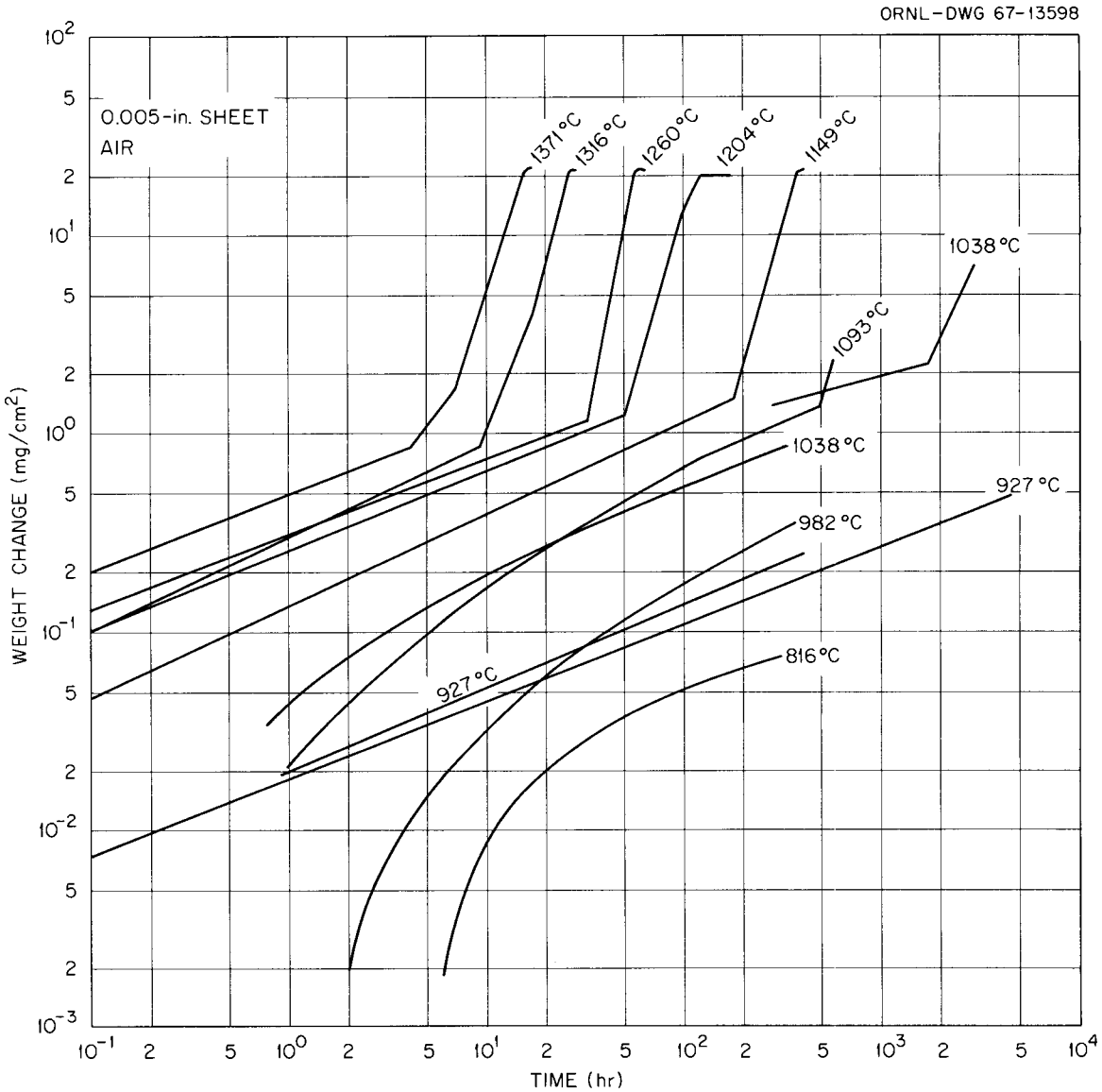

Fig. 23. Oxidation of Type 406 Stainless Steel in Air.

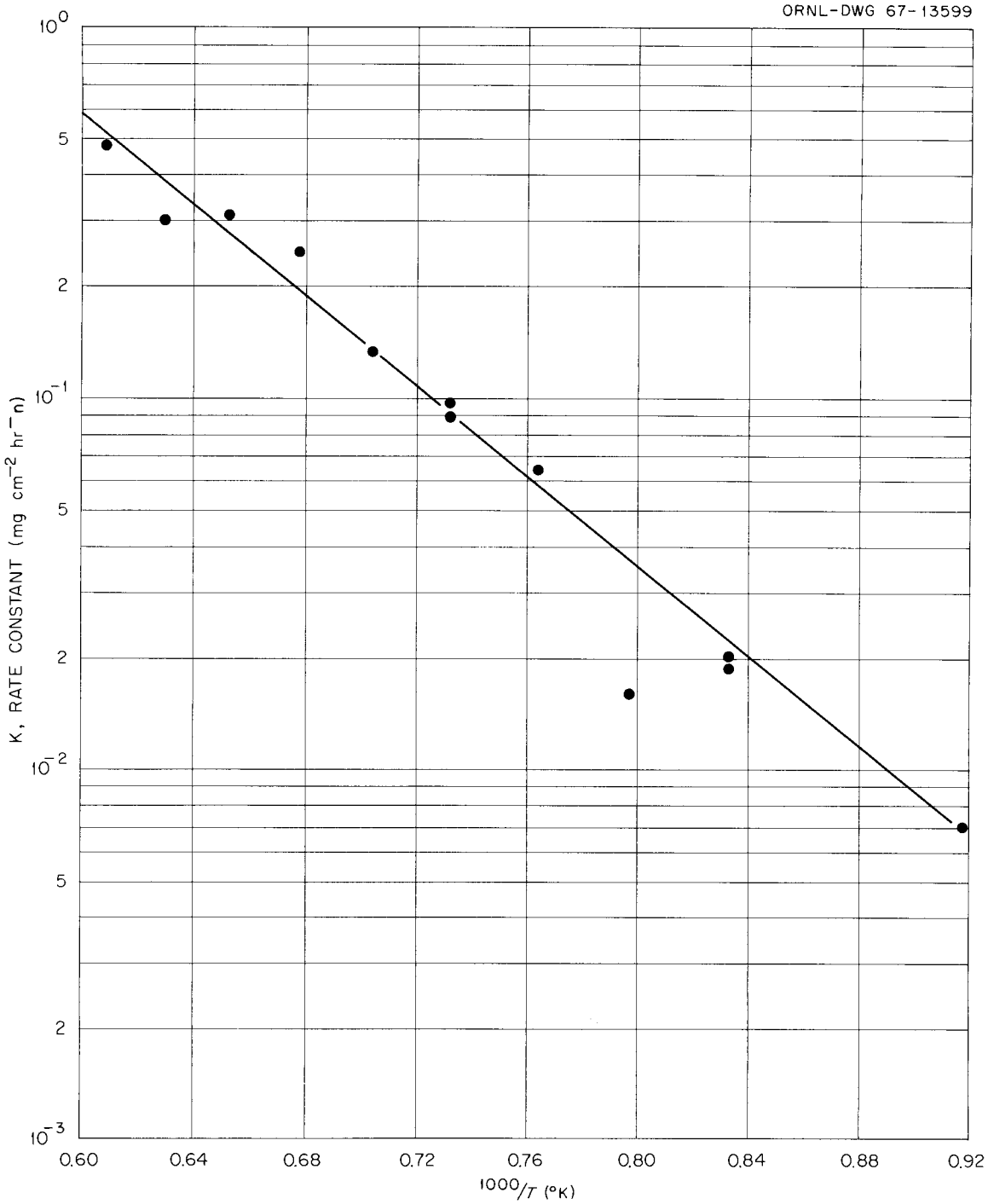

Fig. 24. Variation of the Rate of Oxidation of Type 406 Stainless Steel with Temperature. The constant "n" is approximately equal to 0.5 for this material.

$$K = Ae - \Delta H/RT ,$$

where

A = constant,

ΔH = the activation energy for the rate controlling process, cal/mole,

R = gas constant = $1.987 \frac{\text{cal}}{\text{mole} - {}^\circ\text{K}}$,

T = absolute temperature, °K.

The value of the activation energy for the rate controlling process was obtained from Fig. 24 and was equal to 27,700 cal/mole. This value should correspond with the activation energy for the diffusion of aluminum in iron. However, this quantity does not seem to be available for comparison. The diffusion of aluminum in $NiAl_3$ and Ni_2Al_3 was determined by boundary layer experiments to have activation energies of 27 and 31 kcal/mole, respectively.[12]

The oxide that formed on all specimens examined prior to the increase in rate was α-Al_2O_3. When the weight change reached 1 to 2 mg/cm^2, the rate of oxidation increased and α-Fe_2O_3 was present in the oxide. Assuming that this weight of oxygen reacted with aluminum to form Al_2O_3, essentially all of the aluminum in the 0.005-in.-thick specimen would be consumed. We checked this point by oxidizing a 0.050-in.-thick specimen at 1204°C. Whereas the rate increased in 50 hr for the 0.005-in.-thick sample, the oxidation rate of the thicker sample did not accelerate until 500 hr. Thus, the increase in oxidation rate seems to occur when all the aluminum is reacted to form Al_2O_3 and the times required to cause accelerated oxidation shown in Fig. 23 and Table 7 are correct only for 0.005-in. sheet.

Our results are generally in good agreement with those of Hagel[13] on an alloy containing Fe–24.6% Cr–4.0% Al. However, Hagel noted spalling of Al_2O_3 from samples oxidized at 1200°C. In our study, all oxides were very adherent and no spalling was noted at temperature or during cooling.

---

[12]M.M.P. Janssen and G. D. Rieck, "Reaction Diffusion and Kirkendall-Effect in the Nickel-Aluminum System," Trans. Met. Soc. AIME 239, 1372 (1967).

[13]W. C. Hagel, "The Oxidation of Iron-, Nickel-, and Cobalt-Base Alloys Containing Aluminum," Corrosion 21, 316 (1965).

We investigated the oxidation of this material in flowing CO_2 at 1-atm pressure. The oxidation rates obtained in CO_2 were in excellent agreement with those obtained in air.

Thermal Expansion Measurements

A quartz dilatometer was used to measure the thermal expansion of type 406 stainless steel from 25 to 1000°C. The data were fitted to a quadratic and a cubic model using standard computer techniques. The constants and their errors are listed in Table 8. Statistical analysis showed that the coefficient of the cubic term was significant and that the cubic model better represents the data. The plots of length change versus temperature are shown in Figs. 25 and 26 with a curve drawn for each model. An average value for the coefficient of thermal expansion

Table 8. Coefficients for Thermal Expansion Data

Coefficient	Value	Standard Error
	Quadratic Model[a]	
B_0	-4.025×10^{-4}	6.563×10^{-5}
B_1	9.666×10^{-6}	3.243×10^{-7}
B_2	4.406×10^{-9}	3.168×10^{-10}
	Cubic Model[b]	
γ_0	-6.004×10^{-4}	8.417×10^{-5}
γ_1	1.208×10^{-5}	7.900×10^{-7}
γ_2	-1.562×10^{-9}	1.842×10^{-9}
γ_3	3.903×10^{-12}	1.190×10^{-12}

[a] $Y = B_0 + B_1x + B_2x^2$,

[b] $Y = \gamma_0 + \gamma_1x + \gamma_2x^2 + \gamma_3x^3$,

where
Y = change in length, in./in.,
x = temperature, °C.

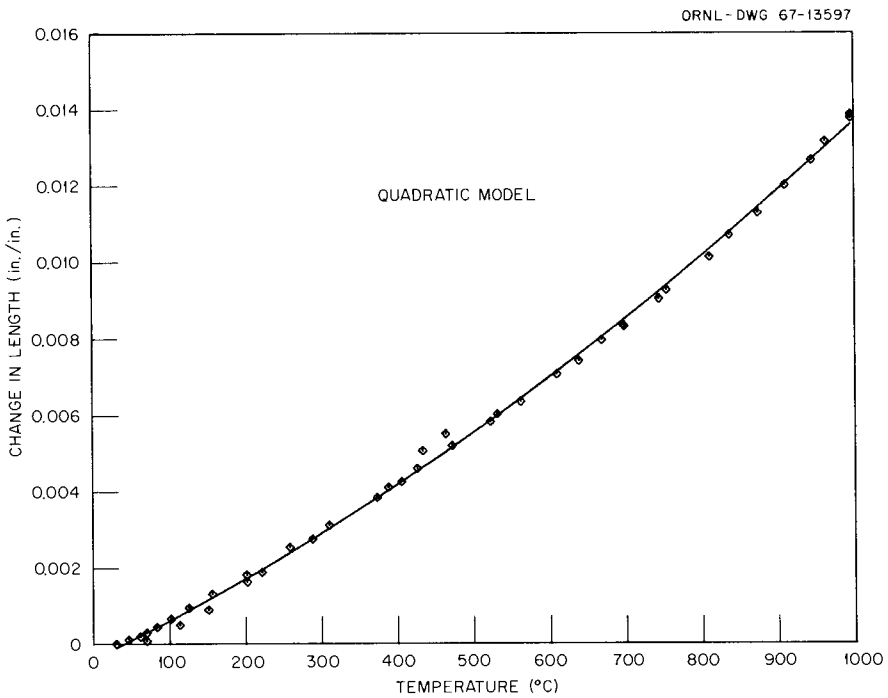

Fig. 25. Change in Length of Type 406 Stainless Steel with Temperature — Quadratic Model.

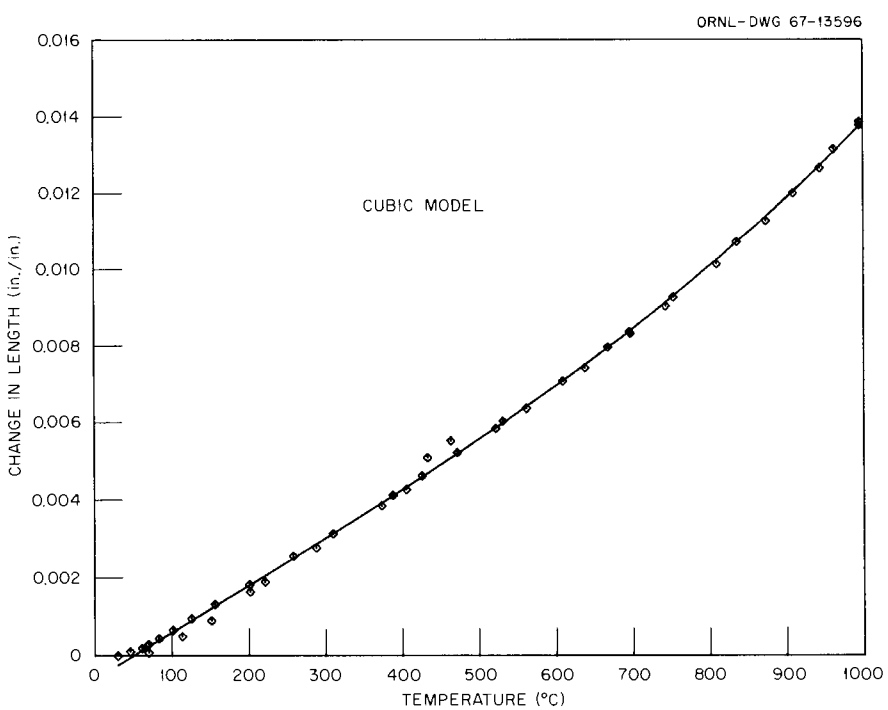

Fig. 26. Change in Length of Type 406 Stainless Steel with Temperature — Cubic Model.

between 25 and 1000°C is $14.2 \times 10^{-6}/°C$. This compares well with a value of 13.1×10^{-6} for type 430 stainless steel,[14] a similar ferritic alloy containing no aluminum.

Welding Studies

The weldability of this material was investigated because of the known susceptibility of ferritic stainless steels to excessive grain growth and high notch sensitivity.[15] Our potential application of this material was for a fuel element cladding and would require that an end closure be made. We butt welded two pieces of 0.020-in. sheet together using type 406 stainless steel filler metal and the TIG welding process. The weld was sound and could be bent sharply without cracking. Photomicrographs of the weld are shown in Fig. 27. The grain sizes in the weld metal and in the heat-affected zone are quite large. Although these results are not extensive enough to warrant a conclusion about the weldability of this material, they do indicate that satisfactory welds can be made in thin sections.

SUMMARY

Our study of this material has revealed a very favorable property — good oxidation resistance — and a very unfavorable property — poor high-temperature strength. These points are illustrated by the comparison of some of the properties of type 406 stainless steel with those of the austenitic type 304 stainless steel in Table 9. The lower coefficient of thermal expansion of the type 406 stainless steel may be important in some applications. The weldability of the ferritic stainless steels is in general inferior to that of the austenitic stainless steels. However, we have demonstrated that satisfactory welds can be made in thin sections. The grain size was stable for long periods of time at 816°C, but grain growth was observed in long-term creep tests at 927°C.

---

[14] Metals Handbook, Vol. I, Properties and Selection of Materials, 8th ed., American Society for Metals, Metals Park, Ohio, 1961, p. 422.

[15] Welding Handbook, 5th ed., sect. 4, ed. by A. L. Phillips, American Welding Society, New York, 1966, p. 64.5.

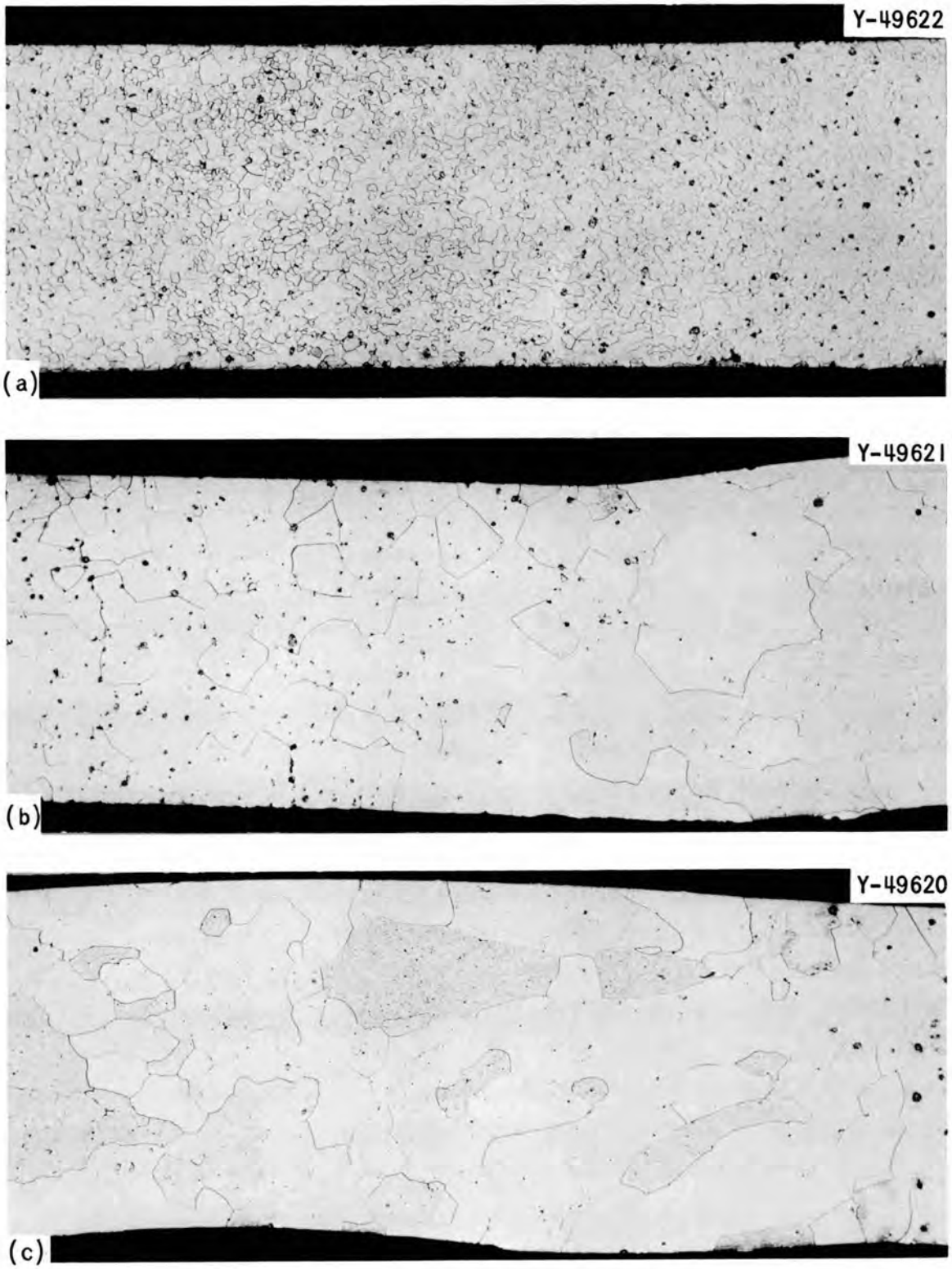

Fig. 27. Microstructures Across a Weld in Type 406 Stainless Steel. (a) Base metal, (b) heat-affected zone, and (c) weld metal. 100×. Etchant: glyceria regia.

Table 9. Comparison of Properties of Types 406 and 304 Stainless Steel

Property	Type 304 Stainless Steel	Type 406 Stainless Steel
Yield strength, psi		
25°C	34,000[a]	58,300
593°C	13,000[a]	29,800
816°C	10,000[a]	7,070
Stress for rupture in 1000 hr, psi		
704°C	9,100[a]	2,400
816°C	3,700[a]	870
927°C		400
Total weight increase in 100 hr in CO_2, mg/cm^2		
816°C	3.0[b]	0.05
927°C	6.0[b]	0.12
982°C	8.0	0.18
1204°C		1.5
Mean coefficient of thermal expansion, $°C^{-1}$		
25 to 1000°C	20.2×10^{-6} [c]	14.2×10^{-6}

[a] Steels for Elevated Temperature Service, U.S. Steel (1949).

[b] H. E. McCoy, "Type 304 Stainless Steel Versus Flowing CO_2 at Atmospheric Pressure and 1100–1800°F," Corrosion 21, 84 (1965).

[c] Metals Handbook, Vol. I, Properties and Selection of Materials, 8th ed., American Society for Metals, Metals Park, Ohio, 1961, p. 422.

Thus, this alloy has several properties that are desirable and others that are undesirable. The data that we have presented should enable one to weigh the various properties in a quantitative manner. This material certainly has its place among the candidate materials for high-temperature applications requiring excellent oxidation resistance.

ACKNOWLEDGMENTS

Several persons were very helpful in completing this study. The creep and tensile tests were run by E. Bolling, the oxidation and thermal expansion experiments were run by B. McNabb, the metallographic work was done by H. R. Tinch, the fitting of the thermal expansion data was done by D. A. Gardiner, the manuscript for this report was prepared by the Metals and Ceramics Division Reports Office, and the drawings were prepared by the ORNL Graphic Arts Department. The microprobe measurements were made by R. S. Crouse. I am particularly grateful to J. R. Weir, C. J. McHargue, and H. Inouye for reviewing this report and making several helpful suggestions.

INTERNAL DISTRIBUTION

1–3. Central Research Library
4–5. ORNL – Y-12 Technical Library Document Reference Section
6–25. Laboratory Records Department
26. Laboratory Records ORNL R.C.
27. ORNL Patent Office
28. G. M. Adamson, Jr.
29. M. Bender
30. G. E. Boyd
31. E. E. Bloom
32. J. H. Coobs
33. R. S. Crouse
34. J. E. Cunningham
35. J. H. DeVan
36. A. P. Fraas
37. J. H Frye, Jr.
38. W. R. Gall
39. R. J. Gray
40. J. L. Gregg
41. B. L. Greenstreet
42. D. G. Harman
43. W. O. Harms
44–46. M. R. Hill
47. H. W. Hoffman
48. H. Inouye
49. R. B. Korsmeyer
50. A. P. Litman
51. R. E. MacPherson
52. W. R. Martin
53–57. H. E. McCoy
58. D. L. McElroy
59. C. J. McHargue
60. R. C. Olson
61. P. Patriarca
62. G. C. Robinson
63. G. Samuels
64. J. L. Scott
65. C. E. Sessions
66. G. M. Slaughter
67. D. A. Sundberg
68. E. R. Taylor
69. D. B. Trauger
70. J. R. Weir
71. G. D. Whitman
72. F. J. Witt

EXTERNAL DISTRIBUTION

73. D. F. Cope, RDT, SSR, AEC, Oak Ridge National Laboratory
74. W. J. Larkin, AEC, Oak Ridge Operations
75. C. L. Matthews, RDT, OSR, AEC, Oak Ridge National Laboratory
76. J. M. Simmons, AEC, Washington
77. E. E. Stansbury, Department of Metallurgical Engineering, the University of Tennessee
78. Laboratory and University Division, AEC, Oak Ridge Operations
79–93. Division of Technical Information Extension